Sudan University of Science and Technology
College of Petroleum Engineering and Technology
Petroleum Exploration Department

Remote sensing and geophysical investigation for geological mapping of the sabaloka inlier, Nile State, Sudan

Prepared by:

- *Abdelelah Hashim Alzubair*
- *Alkhatim Abazar*
- *Mansor Ibrahim Faroug*
- *Mohamed Abdelrahman Magzoub*

Supervisor:
D. Abdelhakam Altayeb

October 2018

الاستهلال

قال تعالى :

(وقل ربي زدني علما)

صدق الله العظيم

DEDICATION

It is our genuine gratefulness and warmest regard that we dedicate this work to our mothers for their kindness and devotion through days and nights.

To our fathers for their sacrifices and encouragement over a number of years for us fulfill what we have achieved.

To our brothers, sisters and families for they created the most hopeful environment to us.

To our university mates for the marvelous and joyful time that we spent with you.
To our dear friends who were always supportive and have a tangible influence on our lives.
To everyone who contributed positively in our lives even with a smile.

Acknowledgments

All Praises be to ALLAH S.W.T the Almighty, for giving us the blessing, the strength, the chance and endurance to complete this work.

We would like to express our very great appreciation to our magnificent supervisor Dr. Abdel-hakam for his valuable and constructive suggestions during the planning and development of this research work. His willingness to give his time so generously has been very much appreciated. for his guidance and support throughout the entire period of this project.

We would like to extend our thanks to our PhDs and lecturers for their patient guidance, enthusiastic encouragement and useful critiques along the university's terms.

We would also like to extend my thanks to Sudan University of Science and Technology. And for everyone and every part who is involved in the consistency of this institution. For the sincerity of their collaboration.

Finally, we are grateful to our parents. We would like express our gratitude for their support and encouragement throughout our study.

Abstract

Sabaloka region comprises some of the old basement rocks in Sudan surrounded with Cretaceous sediments forming an inlier, extending between Khartoum and River Nile States. The study area is located inside this inlier between latitudes N 16 00′ - 16 30′ and longitudes 32 40′ - 33 10′. The digital image processing of Landsat 8 (OLI) oriented to enhance the satellite images to discriminate the boundary between the different rock units in the inlier and their dimensions. Also to explain the structural features at macro scale, recognize and analyze them. The geological perspective of the area is the granulite rocks of Precambrian age exposed within the retrograded gneisses and migmatite rocks which are prevalent in the region of inlier. There are also batholitic rocks of Ban Gadeed, El-Soulik, Ba Bados, and Abu Gedium granites in their foliations. The granulite rocks are two types meta-igneous (enderbite), and meta-sediments (semi-pelitic and calc-silicate).

Field observations, satellite image views, and microscopic studies of microstructures indicate that Precambrian rocks of Sabaloka inlier have orientations of shear foliations of Ban Gadeed-Gamrab Shear Zone (BGSZ) with general trend NW-SE, and it may be the last activity of the Precambrian deformations in the Sabaloka inlier. Ban Gadeed-Gamrab Shear Zone (BGSZ) has affected the Precambrian rocks only and did not affect the younger rocks of the region.

الخلاصة

تحتوي منطقة السبلوقة على واحد من صخور الأساس القديمة في السودان محاطة بالرواسب العصر الطباشيري التي شكلت ما يعرف بحصير السبلوقة القديم ، يمتد هذا الحصير بين ولايتي الخرطوم ونهر النيل حيث تقع منطقة الدراسة داخل هذا الحصير33 -' 40 32. والطول N 10 '. 16 -' 00 16بين خطي عرض30 ' وجهة إلى تحسين صور الأقمار الصناعية للتمييز الحدود بين الصخور المختلفة (OLI) معالجة الصور الرقمية للقمر لاندسات8 ومعرفة أبعادها .أيضا لتوضيح الظواهر التراكيب الجيولوجية في المنطقة لتمييزها وتحليلها. وجهة النظر جيولوجية للمنطقة هو ان صخور الجرانيولايت ما قبل الكمبري تكشف بين صخور النايس والميجماتيت المتراجعة التي تنتشر في منطقة الحصير .أيضا، تحتوي صخور النايس والمجماتيت على متدخلات البان جديد ,السوليك ,البابادوس ,ومتدخل ابوقيدوم في نطاقات تورقها .تنقسم صخور الجرانيولايت في المنطقة الى نوعين الأول ذو أصل ناري يدعى الإندربايت والثاني ذو أصل رسوبي وينقسم الى :أصل شبه طيني والثاني ذو اصل رسوبيات السيليكات الجيريه حيث انه جيوكيميائيا وجد ان لهو اصل ناري ايضا.

الملاحظات الحقليه ,ومشاهد صور الاقمار الصناعية ,والدراسات المايكروسكوبية للشرائح التراكيب الجيولوجية الدقيقة دلت NW-SE الذي يتوجه باتجاه عام BGSZ على ان صخور الاساس بمنطقة السبلوقة تحتوي على تورق نتجة عن قص السبلوقة وهو قد يكون نهاية نشاطات التشوه في عصر ما قبل الكامبري .الملاحظات الحقلية توضح ان نطاق قص البان جديد - الجامراب قد اثر فقط قي صخور القديمة لعصر ما قبل الكامبري ولم تؤثر في باقي صخور اقليم السبلوقة الحديثه.

List of Contents

Dedication……...…II

Acknowledgements……... III

Abstract…….……..... IV

……...…...…...…...…...…...……...……... Vالخلاصة

List of Contents ……..……... VI

List of Table ……..... XI

List of Figures…….….. XI

List of Plates……...……...…... XI

CHAPTER ONE: INTROUDUCTION

1.1 Statement of the problem …… 1

1.2 Objective of the study ……..…..…1

1.3 The studyarea ……..…„…… 2

1.3.1 Location and Accessibility ……..…… 2

1.3.2 Physiography ……..…….…… 2

1.3.2.1 Topography ……..…… 2

1.3.2.2 Climate and vegetation cover ……..…… 3

1.3.2.3 Drainage system …… 4

1.3.3 Population ……..…… 5

1.4 Previous Studies ……..…… 5

CHAPTER TWO: GEOLOGY AND TECTONIC SETTING

2.1 Tectonic Setting 8

2.2 Regional geology 11

2.2.1 Granulite rocks 11

2.2.2 Biotite and migmatite gneisses 13

2.2.3 The granitoid batholiths 14

2.2.4 Late tectonic tholeiitic rocks 15

2.2.5 An-orogenic granites and sub-volcanic sediments 15

2.2.5.1 Abu Tulieh Igneous Complex 16
2.2.5.2 Sub-volcanic sediments 16
2.2.5.3 Sabaloka Igneous Complex 16
2.2.5.4 Sileitat - Es-Sufur Igneous Complex 17

2.2.6 Dykes and Veins 17

2.2.7 Cretaceous sandstone 17

2.2.8 Superficial deposits 18

CHAPTER THREE: METHODOLOGY

3.1 material 19

3.1.1 Digital data 19
3.1.2 Software 22
3.2 Methods 23

CHAPTER FOUR: REMOTE SENSING AND GEOPHYSICAL INVESTIGATIONS

4.1 Introduction 25

4.2 Geological mapping 26

4.2.1 Creation of Meta file 27
4.2.2 Image subset 27
4.2.3 Spatial resolution enhancement 27
4.2.4 Color composite 29
4.2.5 Spectral band ratioing 31
4.2.6 Principal Component Analysis (PCA) 32
4.2.7 Decorrelation Stretching 33
4.2.8 High pass filtering 36
4.2.9 GIS data integration and analysis 38
4.2.9.1 Lithological discrimination 39
4.2.9.2 Linear structures mapping 39

4.3 Gravity Investigations 43

4.3.1 Introduction 43
4.3.2 Basic concept 44
4.3.3 Satellite gravity 45
4.3.4 Satellite Gravity Data Processing and Interpretation 45
4.3.4.1 Bouguer anomaly 46
4.3.4.2 Regional- residual separation 48
4.3.4.2.1 Weighted averaging 49
4.3.4.2.2 Polynomial fitting 50
4.3.4.3 2.5D modeling 53

CHAPTER FIVE: CONCLUSION AND RECOMMENDATIONS

5.1 Conclusions ……..…. 58

5.2 Recommendations ……..…. 59

References ……..…. 60

List of table

Table (3.1): Spectral parameter comparison between Landsat 7 ETM+ and Landsat 8 OLI instruments 20

Table (3.2): Comparison of the capabilities of Landsat, SPOT and Sentinel-2 21

List of figure:

Figure (1.1): Location map of the study area 2

Figure (1.2): DEM image showing the topography of the region 3

Figure (1.3): Drainage system map of study area 5

Figure (2.1): Geological sketch map showing the distribution of the basement units in Sudan and adjacent areas 9

List of Plates

Plate (2.1): Enderbite rocks under microscope 12

Plate (2.2): a, and b: Microscopic view of the calc-silicate rocks 12

Plate (2.3): Microscopic view of biotite gneiss rocks (XPL view) 13

Plate (2.4): Microscopic view of Es Sulik granite 15

CHAPTER ONE: INTROUDUCTION

1.1 Statement of the problem

The Sabaloka igneous complex represents the study area of our graduation project. It forms a part of the Sabaloka Inlier, which is basement rocks of the Precambrian age are surrounded by younger Cretaceous sedimentary rocks. The area attracted the interest of many geoscientists. This is may be explained by the large number of scientific works that have been conducted in the area. Despite this fact, the geological map of the area remained inundated and more enhancements have to be added.

From another point of view, a few geophysical investigations have been conducted in the area. Nevertheless, the total coverage of the acquired data is relatively small. Accordingly, inference about the major structures in the area can hardly be made.

1.2 Objective of the study

The main objectives of the present study are to carry out the following:

- Study the geology of the sabaloka igneous complex making use of the available data (satellite images, gravity data and surface geological information).
- To carryout digital image processing of Landsat 8 OLI data to enhance the different lithological units and structural elements in the area and hence improvement of the visual geological interpretation.
- To integrate the various geological information that would facilitate the production of geological map for the study area.
- Reveal the subsurface geological structures of the area and to produce 2.5D gravity model of the area.

1.3 The study area

1.3.1 Location and Accessibility

The Sabaloka inlier is located in the River Nile State between latitudes: 16° 00` - 16° 52` N and longitudes: 32° 30`- 33° 10`E. It is approximately 80 Km north of Khartoum (Figure 1.1). The area is accessible through Et Tahadi Highway which extends from Khartoum, the capital of Sudan Republic, to Atbara, passing through Sabaloka.

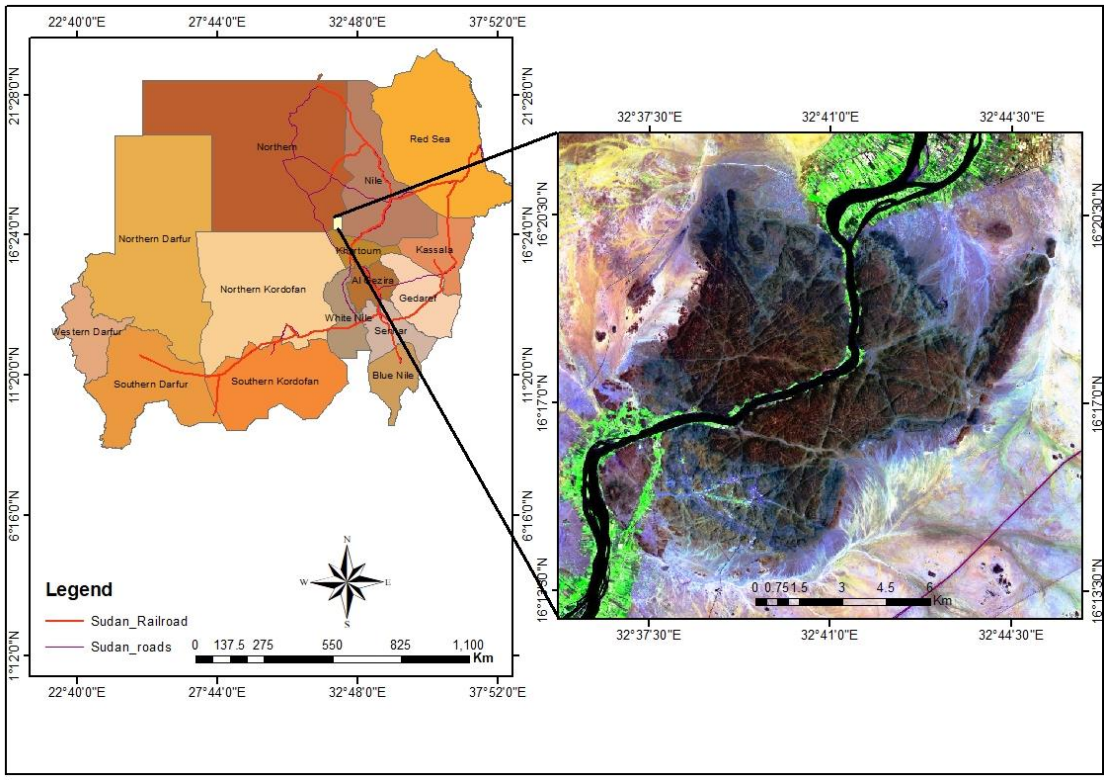

Figure (1.1): Location map of the study area.

1.3.2 Physiography

1.3.2.1 Topography

Topographically, the Sabaloka area is characterized by two distinct terrains Figure (1.2): Sabaloka volcanic plateau with isolated hills; and subdued gneissic peneplain which merges gradually with the River Nile flood plains.

The Sabaloka volcanic plateau has the height that ranges between 450 m to 500 m above sea level, which is surrounded by the micro-granite ring dyke. Also

Jabel Rouwiyan and Jabel Umm Marahik 540 m, 450 respectively above sea level. Jabel Rauwiyan is the highest elevation in the Sabaloka inlier. Isolated hills of moderate relief occur in the peneplain such as Babados, Ban Gadded and Es Suleik. They are composed of granites intruded into the gneisses. The peneplain comprises subdued gneissic outcrops and merges northward with the River Nile flood plains which are formed of silts. The flood plains are narrow and they appear as green colored because of agricultural activities.

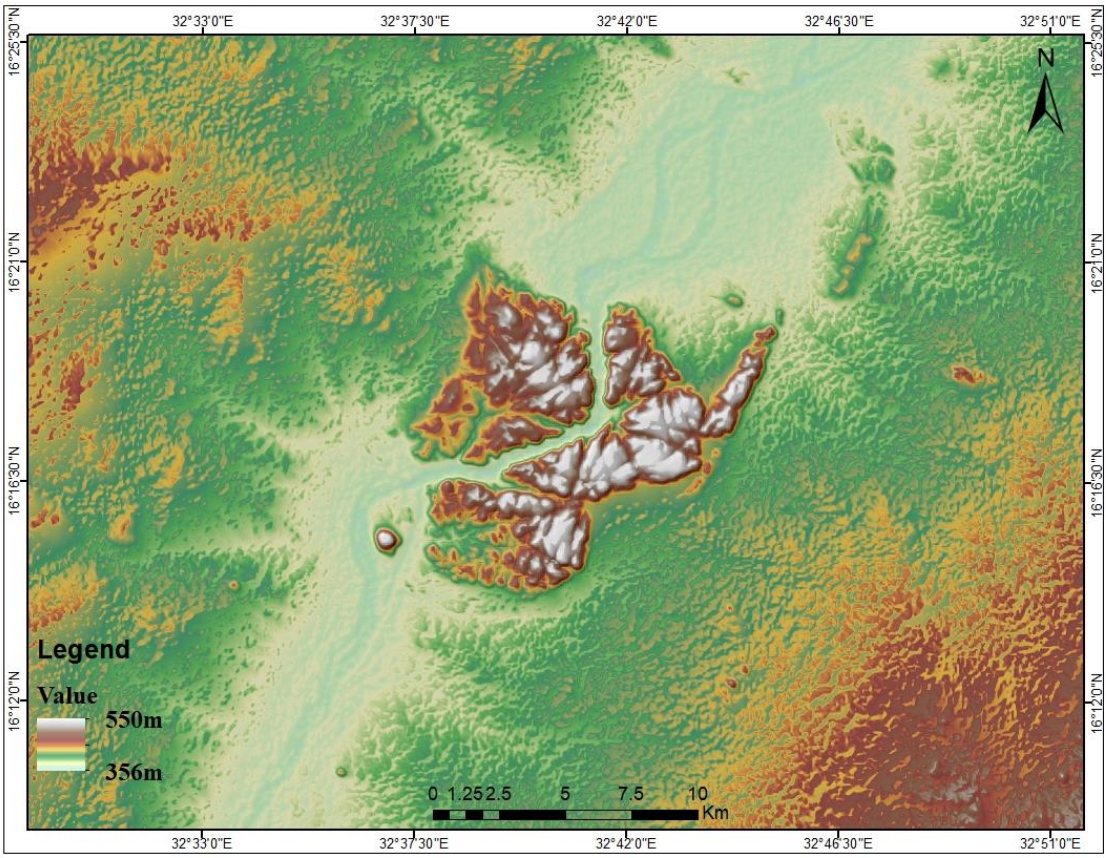

Figure (1.2): DEM image showing the topography of the region.

1.3.2.2 Climate and vegetation cover

Predominantly the semi-desert climate prevails in the Sabaloka region. The dry season is in summer and winter. The northeast dry wind prevails in the period of the month of November to February. The weather in this period is cold. The rest of the year the climate is hot in the period of eight months from March to October and the southwestern wind prevails in this period. The rains pouring

down in the seasons at July-August. The rate of the rainfall is between 100 mm – 150 mm.

The Atmospheric pressure decreased during the daytime and increased at night, inversely proportional to the temperature. The lowest temperature recorded in the month of January and drops to 14 C˚ and the highest in the month of May reach to 42 C˚.

The prevailing climatic condition affected the quality of vegetation cover in the region. The spinose trees called Sial and Mimosa or Sonot of desert environment as well as a few short evergreen trees prevail in the region. They are found concentrated in the seasonal streams. There are some agricultural activities of local peoples along River Nile banks. The area is famous for the farming of onions, potatoes and some vegetables and represents one of the main feeders of the Khartoum market with these products.

1.3.2.3 Drainage system

The River Nile is the main drainage system in the area of the Sabaloka inlier (Figure 1.3). It approximately bisects the volcanic plateau. The others drainage system in the study area is generally characterized by dendritic drainage pattern. It is very simple, all water courses (wadies) cutting into the peneplain of the basement complex and appear to be structurally controlled, where the convergent of the canyons with their branch is angular shape, running towards the River Nile. These wadies supply a great amount of water during the rainy season. Some wadies come from far distance (Butana) like wadi Al Awataib. The main streams flow from west and east toward the River Nile course, such as wadi Abu Gidad, wadi Abu Gedum, and wadi Abu Tulih. Some of these wadies running from Highlands like khor Al Sada, Al sholok, khor Mousa, and khor Al Sagai.

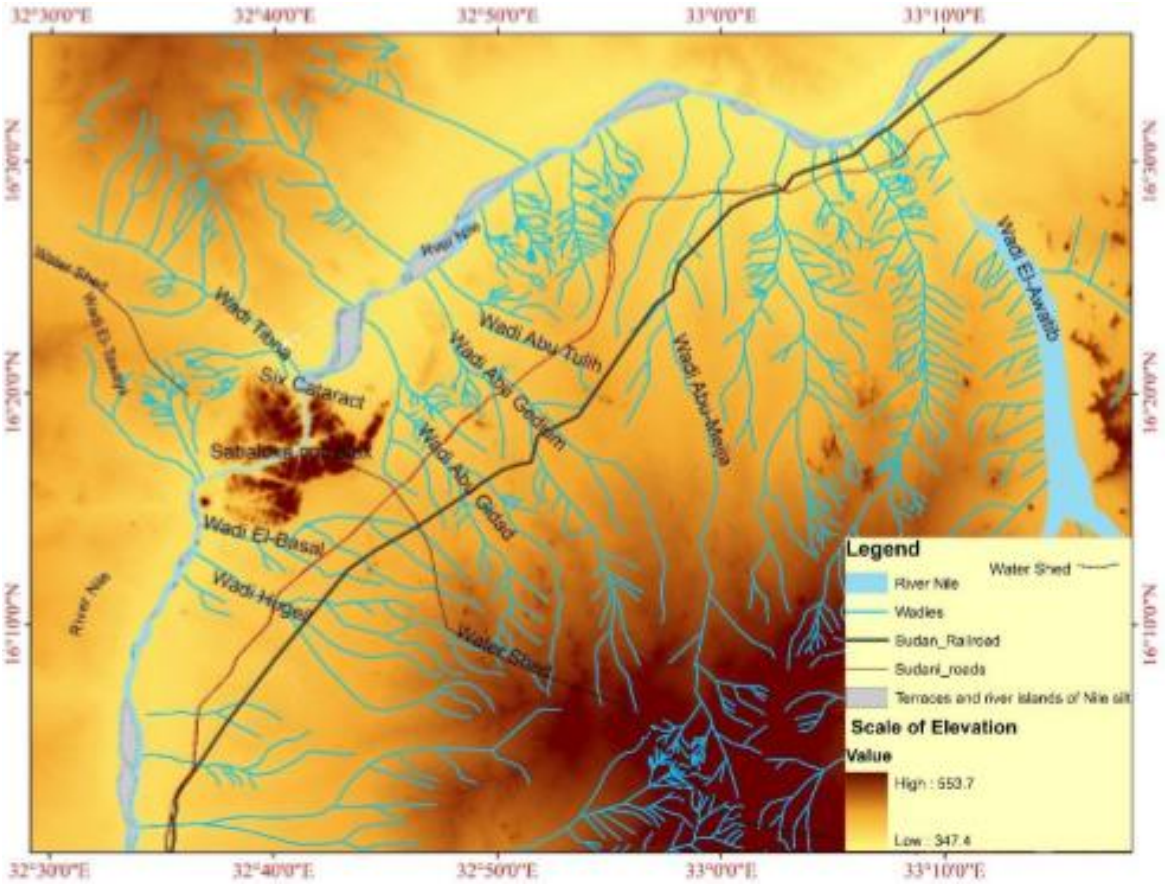

Figure (1.3): Drainage system map of study area

1.3.3 Population

Al Jaalia tribes are considered as aboriginal residents of the area where they live in the region of Sabaloka beside Al shaigia, Al hasaania, and Abdalab. Residents of Sabaloka area living on the River Nile banks, and they work in farming.

1.4 Previous Studies

Delany (1955) and Ahmed (1968, 1977) mapped the complex of Jebel Sileitat Es Sufr, and they found that the complex consists of a pluton of riebeckite granite, volcanic and sub-volcanic rocks, including rhyolite lavas and breccia, micro diorite, pegmatitic syenite and riebeckite quartz syenite.

Delany, (1960) considers the Basement complex in Sudan is Precambrian. Omer, (1975, 1978) give general descriptions of the Cretaceous sediments (the

old term Nubian) between Khartoum and Shendi NE of Sabaloka. Medani (1975) claimed that Jebel Hardan (near Naqa, 45 km E of Ban Gadeed) offers a typical section of what he prefers to consider as the Cretaceous Sandstone Formation of Sudan.

Dawoud (1970) and Almond (1977, 1980) showed that in the Sabaloka basement inlier granulitic facies rocks occur as lenses, bands and irregular bodies. Almond (1977) mapped the Sabaloka igneous complex and found the complex has a volcanic phase that consist mainly of rhyolites, agglomerates, and ignimbrites forming a plateau and intruded by elliptical ring dyke of micro-granite.

Almond (1980) analyzed the rocks of Sabaloka Cauldron and calculated that they are poorer in Na_2O and have lower Na_2O/K_2O ratios than of Nigerian granites. Almond (1980) also found the gneiss assemblage contains evidence that an early granulite facies metamorphism occurred and followed by retrogression into the amphibolite facies.

Berry and Whiteman (1968) considered the Sabaloka complex an inlier, the term exhumed monadnock or inselberg is more appropriate, as the Sabaloka complex is not directly surrounded anymore by Nubian sandstone. Also they are correct and supposing that the course of the Nile was superimposed above, and thus its position in relation to Jebel Sabaloka is entirely accidental.

Kroner et al. (1987) dated the granulite facies metamorphism in Sabaloka area as occurring around 720 Ma and this age is similar to the Mozambique Belt which extends northward to include Sabaloka and forms a geographical and metamorphic bridge between the Pan-African arc accretion green schist assemblage of the Arabian Nubian Shield to the east and Pre-Pan-African higher grade metamorphic terrain to the west.

Dawoud and Sadig (1988) indicated the thrusting by structural and gravity data as the major cause of uplift for the granulite rather than by erosion only. The geophysical measurements carried by Sadig and Ahmed (1989) across selected complexes of younger granite from Sudan indicate different gravity signatures, where the Sabaloka complex is characterized by low Bouguer gravity values. Dawoud and Dobrik (1993) discussed the P.T condition of PanAfrican granulite facies metamorphism in Sabaloka inlier.

CHAPTER TWO: GEOLOGY AND TECTONIC SETTING

2.1 Tectonic Setting

The Sabaloka rocky region of the Precambrian rocks is situated near the northeastern margin of ancient Africa itself only a part of an enormous super continental margin orogenic belt named East Africa Orogeny (EAO) (Stern, 1994; Figure 3.1). The ophiolites, granulite, and structures of the EAO are fossil fragments of a Neoproterozoic Wilson cycle, representing the opening and closing of an ocean basin that lay between the older crustal blocks of East and West Gondwanaland (Stern, 1994). The Wilson cycle of the EAO beginning with rifting, and the evidence for rifting maybe preserved in sedimentary successions in the EAO that have been interpreted as passive margin deposits in Kenya (Vearncombe, 1983, Key et al., 1989, Mosley, 1993) and in Sudan (Kröner et at., 1987). Many of these collisions were between the arcs, as the oceanic crust between them was subducted, but a few collisions involved the addition of arcs and arc-complexes and continental micro-plates to the African margin (Almond et al., 1993).

The collisions led to low grade metamorphic facies in Nubian Arabian Shield (ANS) increasing in grade of metamorphism toward west in Bayouda Desert and reached the maximum in Sabaloka area (Dawoud, 1988). The sediments from Sudan were metamorphosed to granulite facies located in Sabaloka inlier at about 720 Ma (Kröner et al., 1987).

The crustal thickening produced pressure with about 6 to 8 Kbar and temperature with range between 600 – 800˚C (Dawoud and Dobrik, 1993) that indicate the metamorphism in deep-seated root of this continental crust with depth between 20 - 30 Km, which led to metamorphose that complex rocks of old continental shelf in this depth at granulite facies. The Sabaloka granulite facies metamorphism, dated at about 700 Ma by Kröner et al. (1987) may have

taken place in the root zone of an island arc at about this time, and in a dry environment. Also Küster et al. (2008) dated by geochronological and isotopic study of granitoid rocks from the eastern boundary of the Saharan Metacraton indicate that the Bayuda Desert and Sabaloka region records orogenic events starting in the early Neoproterozoic (920 -900 Ma: Bayudian event) and ending during late Pan African times (ca. 600–580 Ma). This age is similar to the Mozambique belt which extends northward to include Sabaloka area (Kröner et al., 1987).

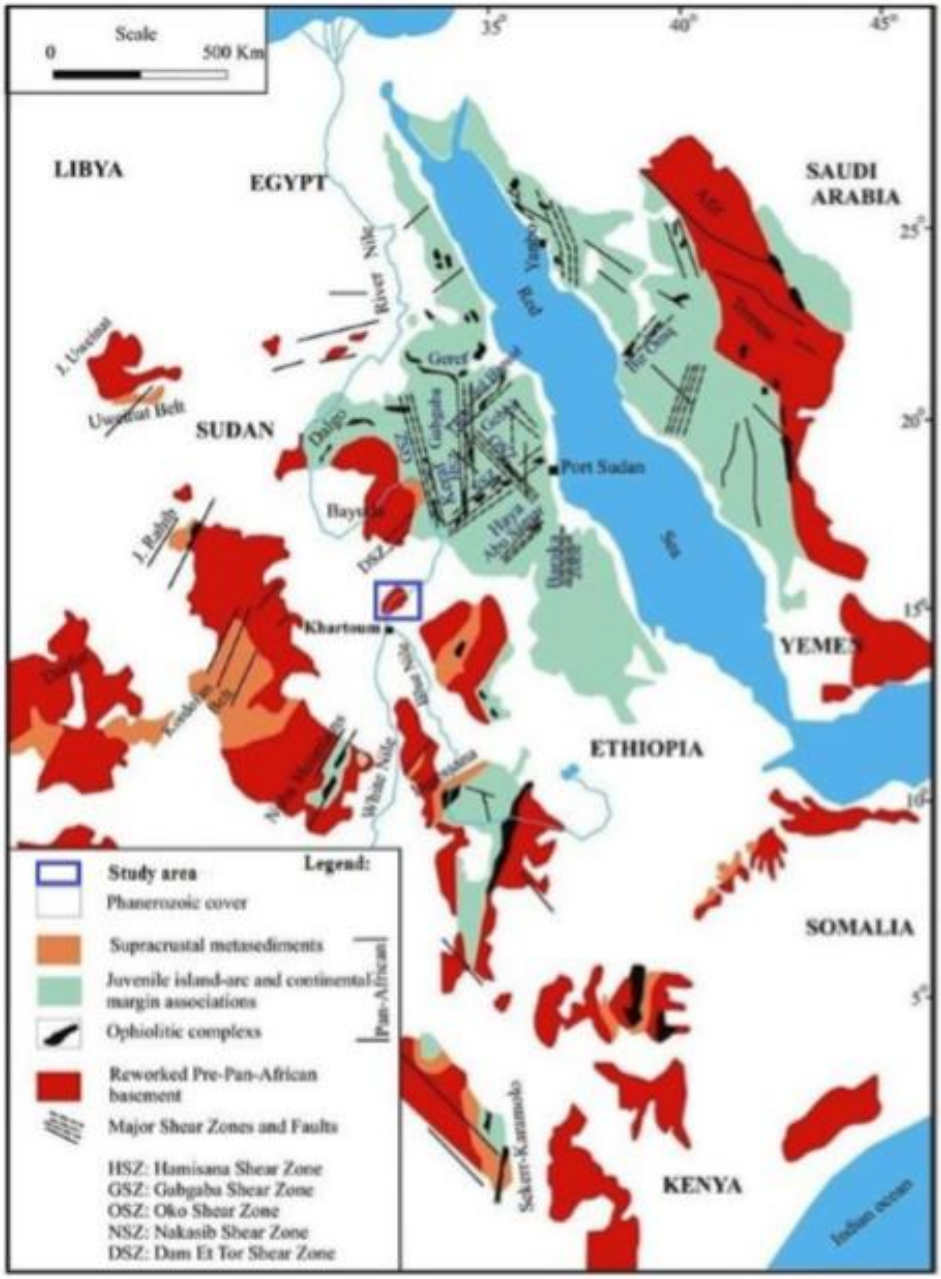

Figure (2.1): Geological sketch map showing the distribution of the basement units in Sudan and adjacent areas (Modified after Abdel Rahman, 1993).

The uplifting of granulite terrane was accompanied by hydration and retrogression under amphibolite facies condition that formed gneisses and migmatites rocks. The scale time is evident at Sabaloka between the granulite facies metamorphism 720Ma and retrogression migmatites possibly subsequent to uplifting 570Ma (Kröner et al., 1987). This conversion of many dry granulite to amphibolite facies gneisses which occurred about 150 Ma later involved an abundance of hydrous solutions, and introduction of water into these hot dry rock caused extensive partial melting (Almond et al, 1993). This resulted in migmatization and the formation of small granite plutons, like Ban Gadeed, Babados, Es Suleik, and Abu Gedium. These events may have accompanied accretion of the arcs, and are assigned to the end of the Precambrian (Kröner et al., 1987).

The strike slip tectonic movement of Ban Gadeed-Gamarab Shear Zone (BGSZ) which effected the Precambrian rocks of Sabaloka inlier is indicated by Ban Gadeed interfolial fold of Z-shape, and porphyroclasts of feldspar and quartz of augen gneiss, and miner interfolial folds in Al Gamarab area. Also Abu Geidum shear (P-shear zone) supports that this shear is dextral ductile shear zone. This horizontal tectonic movement may have occurred after emplacement of older granites of Sabaloka inlier, and before Abu Tulieh, Sabaloka, and Sileitat Es-Sufur igneous complexes, because the shear has not affected these igneous complexes (Elyas, 2016).

Tectonic stability was, however, locally punctuated by outbursts of igneous activity which, at long intervals, built up felsic volcanoes rising above the gneissose peneplain. The positions of these volcanoes are now marked by younger granite complexes, of which there are over 100 in Sudan alone (Vail, 1985). At Sabaloka inlier the igneous activities are different in ages recently defined by isotope dating of the complexes of Tuleih, the Cauldron complex of Sabaloka and Sileitat Es-Sufur (Almond et al., 1980).

The most prominent post-Cretaceous structure in the Sabaloka area is the Umm Marahik fault and its associated transtensional basins. The principal displacement on this fault is recorded by 2 km, dextral shift of the sub-vertical structures of the Cauldron complex ring-fracture zone (Almond et al., 1980). It may be rejuvenation of old fracture has a bearing on Ban Gadeed-Gamarab Shear Zone (BGSZ; Elyas, 2016). A part from the E-W strike-slip faults, there are also a number of normal faults of small throw trending approximately N-S. Several of these faults can be seen offsetting the Nubian basal unconformity to the S and SE of Ban Gadeed (Almond et al., 1980).

2.2 Regional geology

The area around the Sabaloka igneous complex has been the subject of many research works and a litho-stratigraphic sequence has been adopting by the previous workers. This has been also adopted in this work, with some modification. Brief description of the various geological units is provided in the following sections:

2.2.1 Granulite rocks

The oldest rock unit in the inlier, occurs as irregular patches and bands ranging in size from a few meters to more than 500 meters across within biotite gneisses and migmatite rocks (Almond, 1980). These rocks are of two types regarding the origin: met-igneous (2.1) and meta-sediments (2.2) .The meta-sediments (para-granulite) are divided to meta-semi-pelitic rocks existing in the inlier as patches. The calk-silicate rocks are the second type of para-granulite also existing as patchy outcrops. In hand specimen, it has dark color and waxy luster characteristic of granulite rocks (Almond, 1980). Kröner et al. (1987) dated this rocks at about 700 Ma, and suggests that they may have taken place in the root zone of an island arc at about this time, and in a dry environment. The granulite

may have been metamorphosed at depth exceeding 25 Km and then later elevated along a thrust (Dawoud and Dobrik, 1993).

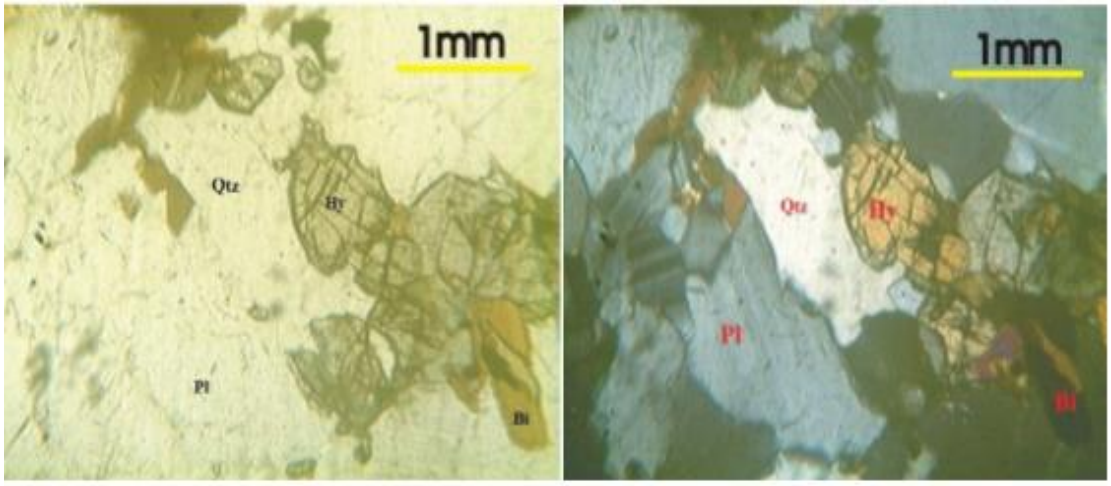

Plate (2.1): Enderbite rocks under microscope where (a) is ppl view and (b) is xpl view. Qtz=Quartz, Hy= Hyperthene, Bi=Biotite, and Pl= Plagioclase

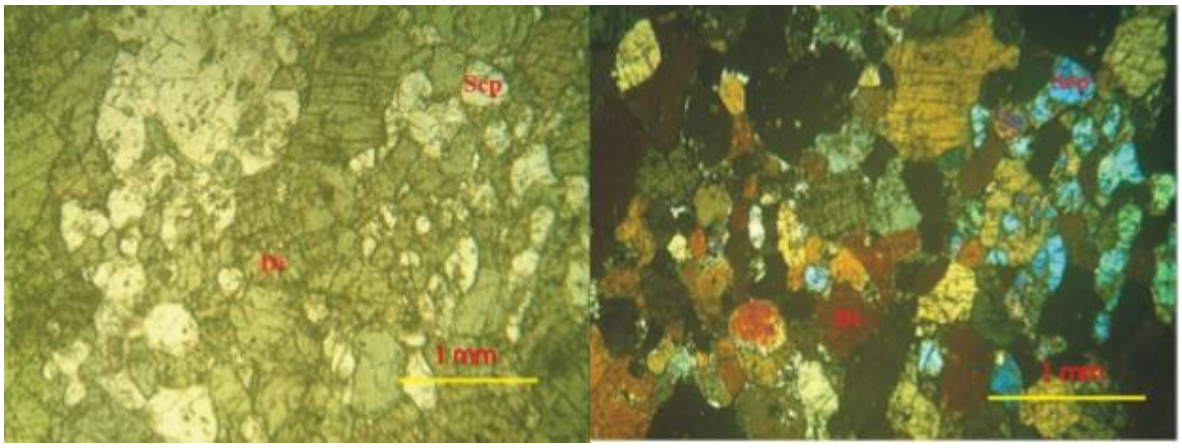

(PPL view) (a) (XPL view)

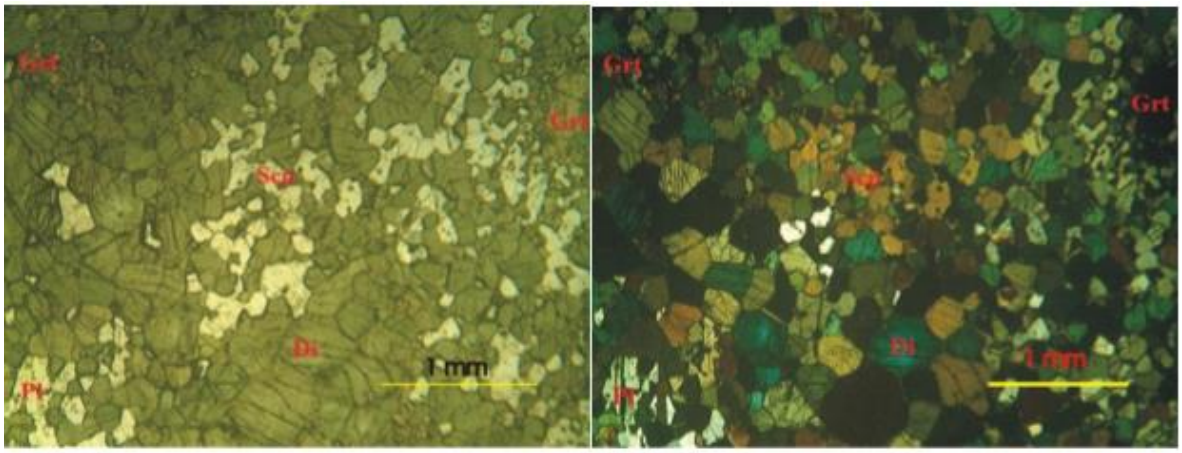

Plate (2.2): a, and b: Microscopic view of the calc-silicate rocks, where: (Di) diopside, (Scp) scapolite, (Pl) plagioclase, and (Grt) garnet

2.2.2 Biotite and migmatite gneisses

Biotite and migmatite gneisses are the country rocks. They have patches of granulite rocks, batholithic older granites and younger igneous complexes with their foliation. They are retreat from granulite facies to amphibolite facies. The origin of the retrograded rocks is para-granulite gneiss rocks of semi-pelitic sediments, with garnet considered as an indicator of the retrogressive metamorphism. Also the retrogressive metamorphism is indicated by the gradual change from a two pyroxene gneiss, through rocks containing both granulite and amphibolite facies assemblages to typical amphibolite facies assemblages in the same outcrop (Almond, 1980). Dawoud, (1970) noted no obvious structural differences between the granulite and the enclosing gneisses and migmatites (Plate 2.3).

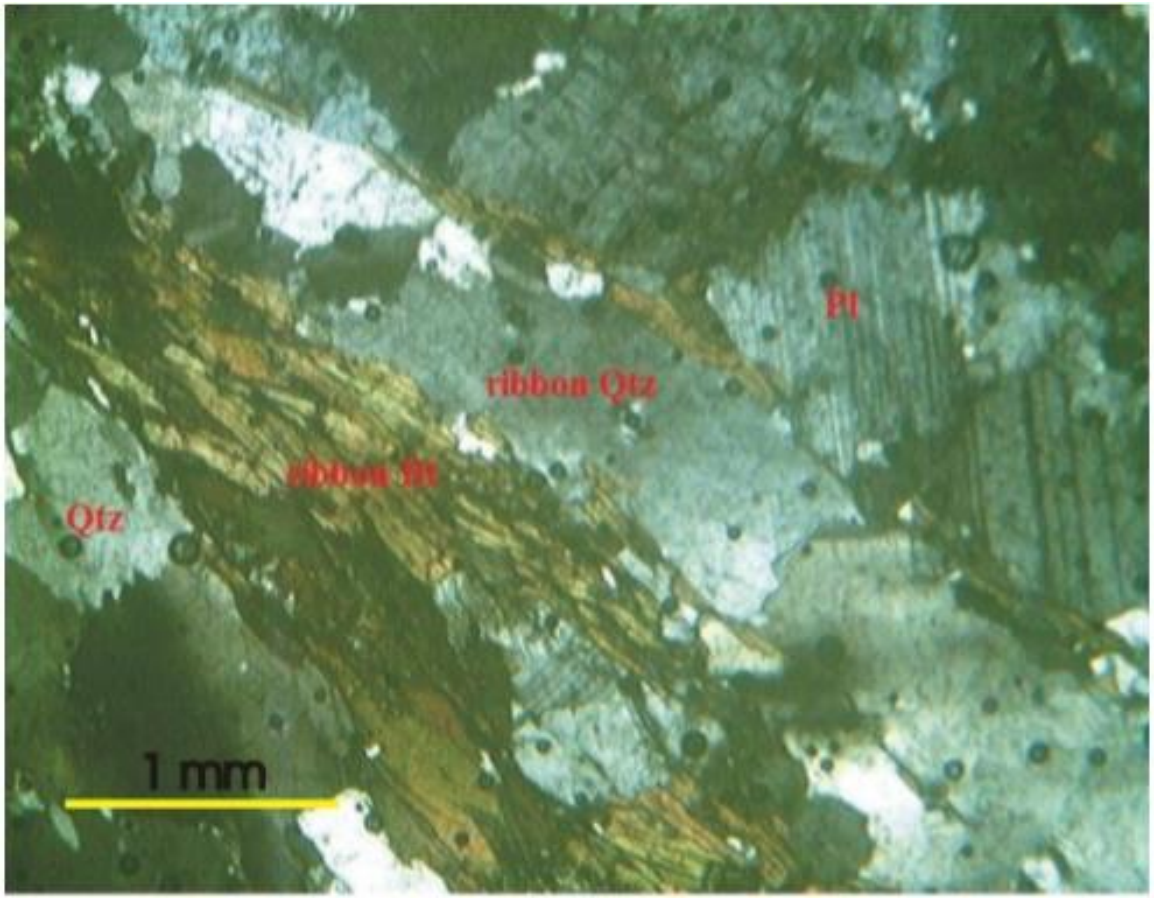

Plate (2.3): Microscopic view of biotite gneiss rocks (XPL view). Qtz= Quartz, Pl= Plagioclase, and Bio= Biotite

2.2.3 The granitoid batholiths

The migmatite rocks are characterized by the development of anatactic granitiod bodies carrying large porphyroblastic K-feldspar and garnet (Dawoud et al., 1993). They are characteristic of the basement complex of Sabaloka inlier, Ban Gadeed, Es Suleik, Babados, and Abu Gedium plutons. These represent different stages of anataxis and include synorogenic foliated granitoids, partially foliated granitoids and weakly or non-foliated granitoids (Dawoud et al., 1988). Some varieties only show relict ghost foliation, migmatite border zones, and variable relict gneisses with no distorted foliation with respect to the prevailing regional foliation.

The older granitoids have a broad concordant relation with the enclosing gneisses and develops foliation particularly at the margins, but dykes of the same bodies cut across the gneisses and the earlier anatexis granitoids. With some of this type of granite, particularly the Es Suliek batholith, lenses and bands of retrogressed amphibolites are abundant probably as rafts (Almond, 1980). Ban Gadeed granite considered as the last stage of migmatization which is typical anataxis granite formed by partial melting. This is evidenced by the presence of garnet in some part of the intrusion, absence of sharp intrusive contact and the presence of ghost foliation inherited from the parent rock.

Es Suleik and Babados are syn-orogenic S-type granite Plate (2.4). They are broadly concordant with exposed dykes cutting sharply across the older structure. The two plutons are composed of adamellite rocks containing between 10 - 35 percent feldspar in addition to hornblende and biotite. The contact of Suleik and Babados plutons are well defined in most phases, but locally are marginal migmatite (Almond et al., 1993). Abu Geidum granites are post-orogenic, strongly discordant and have very weak internal foliation K-feldspar porphyroblast is absent. They are dark in color and contain angular xenoliths (Dawoud, 1970, 1980; Almond, 1980).

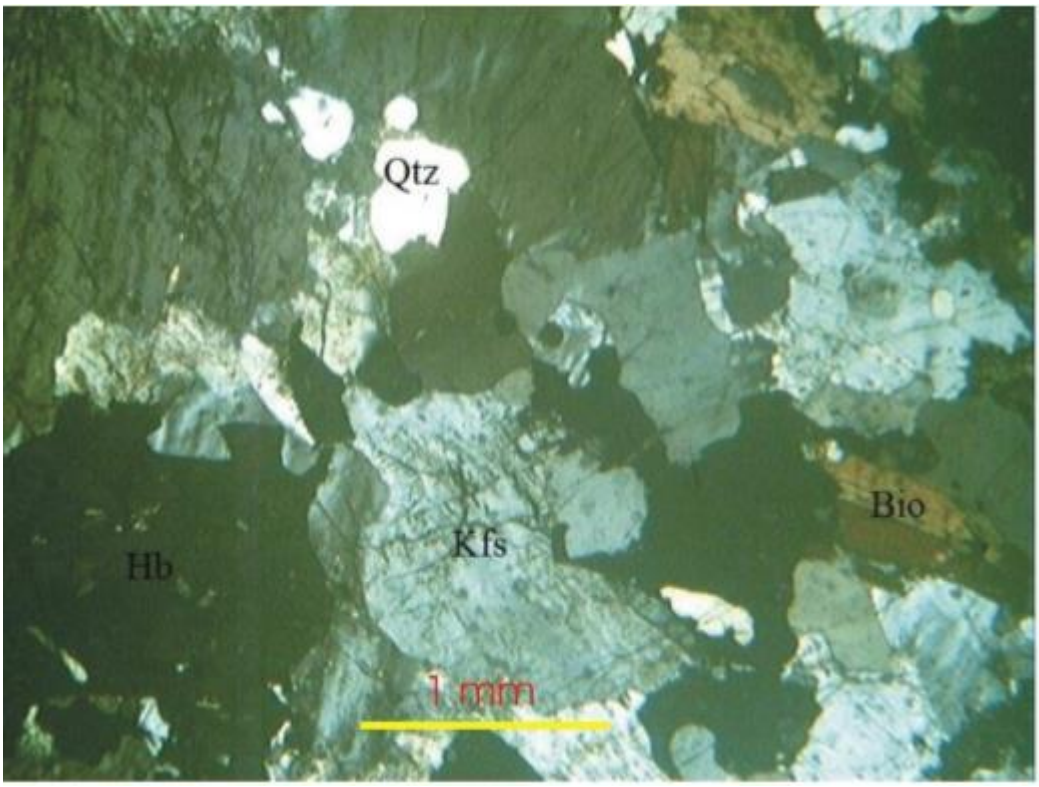

Plate (2.4): Microscopic view of Es Sulik granite

2.2.4 Late tectonic tholeiitic rocks

Gabbro is a distinctive feature of the Ban Gadeed area. These basic rocks are primarily of tholeiitic affinity and, being mildly metamorphosed and weakly deformed (Almond et al., 1993). Dawoud (1970) refers to it as a meta-gabbro, and mapped several such small intrusions along a line parallel to the felsite dyke swarm. Several of these dykes cut the gabbro. The gabbro is a late tectonic member of the basement complex (Almond et al., 1993).

2.2.5 An-orogenic granites and sub-volcanic sediments

The A-type granite suites vary in composition from quartz syenites to per-alkaline granites and their respective volcanic equivalents. These suites are emplaced into non-orogenic settings both within the plate and along plate margins during the waning stages of subduction-zone related magmatism (Eby, 1990). As defined by Loiselle and Wones (1979) the A-type granite occurs

along rift zones and within stable continental blocks. In Sabaloka inlier there are three complexes of an orogenic A-type granite.

2.2.5.1 Abu Tulieh Igneous Complex

Abu Tulieh Complex is oldest igneous complex in the inlier, with an age of 465 ± 14 Ma in the middle Ordovician (Harris et al., 1983; Klemenic, 1987). The predominant rocks are buff colored moderately coarse syenites with enclosures of country rocks and intrusions of microgranites (Almond et al., 1993).

2.2.5.2 Sub-volcanic sediments

An upward-fining sequence of clastic sediments about 75 m thick underlies the volcanic rocks on the NW contact of the Mica granite in the western part from Sabaloka igneous complex. The sediments strike NE and dip steeply SE, resting with strong unconformity upon Basement gneisses, which strike NW (Almond et al., 1993). The sedimentary sequence begins with quartz conglomerates and passes upwards through flaggy and micaceous sandstone into black shale. All these rocks have been strongly metamorphosed by granite, and some of the pelitic hornfels contain andalusite and cordierite (Almond et al., 1993).

Considering their conformable relation to the overlying volcanic rocks and the radiometrically determined lower Devonian age of the Cauldron complex, it seems likely that the sediments are also of early Devonian age, and it is unfortunate that their metamorphosed condition makes it unlikely that they will yield any fossils (Almond et al., 1993).

2.2.5.3 Sabaloka Igneous Complex

Sabaloka igneous Complex is younger than Abu Tulieh complex, with an age of 383 ± 14 in the lower Devonian (Harris et al., 1983). The complex has thin sheets of trachytic-basaltic lava, which is the beginning of the volcanicity in the complex, early rhyolite lava, and volcano pyroclastic rocks. It is fining upward beginning by agglomerate, light ignimbrite, dark ignimbrite, and ending with a

thin unit of bedded tuffs. The last volcanic unit in Sabaloka complex is upper rhyolite which came finally and all the complex rocks are predominantly aluminous to slightly per-aluminous (Almond et al., 1993).

2.2.5.4 Sileitat - Es-Sufur Igneous Complex

The Sileitat Es-Sufur igneous complex lies on the eastern side of the Nile valley some 30 km N of Khartoum town. This is younger than Sabaloka igneous Complex. The age of this rock is middle Jurassic (169 ± 2 Ma; Klemenic, 1987). The complex comprise riebeckite granite, syenite, and micro syenite, and it is peralkaline (Almond et al., 1993).

2.2.6 Dykes and Veins

These are found as low outcrops from quartz veins, felsite dykes, blue quartz micro-granite and some dolerite dykes. They are 10 m to several hundred meter in length. Quartz veins are ridges in appearance extending 40-250 m and (6-13) m in width. Felsite dykes are fine textured and represent the last stage of granitization, some of them are faulted, like Ban Gadeed area which has felsite dykes swarm (including an unusual dyke composed of glass). Blue quartz micro-granite is porphyritic texture, and attains a width of 20 m and is of microgranite containing phenocrysts (up to 2 cm) of blue-tinted quartz and pink-white feldspar. In fact, later isotopic dating has revealed a range from lower Ordovician to middle Jurassic for the Sabaloka area alone, and a recent K-Ar date on a glass dyke suggests the possibility of limited activity until the end of the Cretaceous (Almond et al., 1989).

2.2.7 Cretaceous sandstone

The Cretaceous sandstone is the new name to the old name Nubian Sandstone Formation (Prasad et al., 1986). Because the term Nubian described the concept of the location only and it does not benefit to describe another unit with the same rocks in any location, but the Cretaceous is a term describing all sediments

that have depositional time in any location in the world. Within the Sabaloka inlier, there are at least five small outliers of the Cretaceous rocks, for example Jebel Umm Marahik, Jebel Rauwiyan, and Jebel Ganam.

The Cretaceous sediments of Jebel Umm Marahik are similar to those seen at Jebel Rauwiyan, though less strongly cemented and more ferruginous. Cretaceous Sandstones are usually bedded and flat lying or very gently dipping. It is composed of conglomerates, sandstone, and mudstone (Omer, 1975). Umm Marahik has silicified sandstone which formed by the movement of strike-slip fault know as Umm Marahik fault, where that movement led to form the silicified sandstone from partial melting of quartz which acted as cementing material for grains of quartz.

2.2.8 Superficial deposits

The superficial deposits in Sabaloka area include Nile silts, alluvial fans, aeolian sands, lag gravels, and wash-zone sands. They are Quaternary period sediments. River Nile silt is found in and along the line of the River Nile Bank. Alluvial fans border the volcanic plateau and have spread a sheet of igneous gravel over the adjacent pediment of gneiss, and extensive alluvial fans sweep down from the foot of the Scarp towards the River Nile, skirting the small Cretaceous hill of Jebel Umm Marahik. Aeolian sediments are fine sands found in foots of mountains in the area. They are considered windbreaks deposited at pediment of gneiss, and low areas in the region that are blocked. In most part of the area bedrock is thinly covered by lag gravels and gritty sands.

CHAPTER THREE: METHODOLOGY

In order to fulfill the objective of the present study, different materials and methods have been utilized.

3.1 material

Different types of materials were used in this research to assist in fulfilling the purposes of this study.

3.1.1 Digital data

The following materials were made available for the present study:

- Landsat 8 OLI (Operational Land Imager), path 173/raw 45, that includes
- 11 bands, from which bands 2, 3, 4, 5, 6 and 7 were used.
- Sentinel MSI image obtained from the European Space Agency (ESA), with spatial resolution of 10 m, which was used to enhance the spatial resolution of the Landsat 8 OLI multispectral image.
- Digital Elevation Model dataset (N16-E32) in raster format with 90m spatial resolution, obtained from the USGS.
- Satellite gravity grid data which was originally provided as Free Air Anomaly (FAA) delivered together with the elevation data for each point. The data was obtained from the Satellite Geodesy at the Scripps Institution of Oceanography, University of California San Diego.

Landsat 8 OLI data

Landsat 8 OLI (Operational Land Imager) considered as an enhanced version of the Landsat-7 ETM+ system .The satellites track the changes in agricultural output, urban sprawl, water consumption, and other land-use trends. It carried two advanced sensors, The Operational Land Imager (OLI) and the Thermal Infrared Sensor (TIRS).

The data of these two sensors are merged into a single data stream and together the (OLI) and (TIRS) instruments on LDCM replace the ETM+ instrument on Landsat-7 with significant enhancements. They produce a complete picture of the Earth's surface every 16 days. The multispectral and moderate resolution OLI instrument has similar spectral bands to the ETM+ in Landsat 7 as a blue, green, red, NIR, SWIR-I and SWIR-II channels with 30-meter spatial resolution and band 8 is panchromatic with 15-meter spatial resolution. (Table, 3.1): It includes new coastal aerosol (band 1) and cirrus detection (band 9) and they also have the same 30-meter spatial resolution, though it does not have a thermal infrared band. While the Thermal Infrared Sensor (TIRS) has 2 spectral bands (10-11) in thermal portion of the spectrum, with 100-meter spatial resolution, this sensor monitors the temperature of the Earth's surface.

Table (3.1): Spectral parameter comparison between Landsat 7 ETM+ and Landsat 8 OLI instruments (http://www.jpl.nasa.gov)

Parameter	**Landsat 7 ETM+**			**Landsat 8 OLI**		
	Band	***µm***	***GSD (m)***	***Band***	***µm***	***GSD (m)***
Spectral bands				**1(Blue)** coastal	0.43-0.45	30
	1 (Blue)	0.45–0.52	30	**2 (Blue)**	0.45–0.52	30
	2 (Green)	0.52–0.60	30	**3 (Green)**	0.52–0.60	30
	3 (Red)	0.63–0.69	30	**4 (Red)**	0.63–0.68	30
	4 (NIR)	0.76–0.90	30			
				5 (NIR)	0.84-0.88	30
				9 (cirrus)	1.36-1.39	30
	5 (SWIR1)	1.55–1.75	30	**6 (SWIR1)**	1.56-1.66	30
	7 (SWIR2)	2.08–2.35	30	**7 (SWIR2)**	2.10-2.30	30
	8 (PAN)	0.500 - 0.680	15	**8 (PAN)**	0.500 -0.680	15
	Thermal Band			**LDCM TIRS**		
	6 (TIR)	10.4–12.5	60	**10 (TIR1)**	10.3-11.3	100
				11 (TIR2)	11.5-12.5	100

Sentinel 2A

The Global Monitoring for Environment and Security (GMES) Sentinel 2A mission ensures the continuity of services that rely on multispectral higher solution optical observations over global terrestrial surfaces. The mission has been designed as a dependable multispectral Earth observation system that will ensure the continuity of Landsat and SPOT observations and improve the availability of data for users (Table 3.2).

Sentinel 2A is a multispectral Earth observation system featuring a Multi-Spectral Instrument (MSI) with 13 spectral bands ranging from the visible and near infrared (VNIR) to the Short-Wave Infrared (SWIR). The spatial resolution varies from 10m to 60m, depending on the spectral band, with a 290km field of view. This unique combination of high spatial resolution, wide field of view and broad spectral coverage represents a major step forward compared with other multispectral missions (Figure 3.1)

Table (3.2): Comparison of the capabilities of Landsat, SPOT and Sentinel-2

Sensor	LANDSAT 1-7	SPOT	SENTINEL-2
Instrument principle	Whiskbroom	Pushbroom	Pushbroom
Earth coverage(days)	16	26	5
Swath width (km)	185	2 x 60	290
Spectral bands	7	4	13
Spatial resolution(m)	30, 60	2.5, 10, 20	10, 20, 60

The Sentinel 2 MSI has the following channels (Bertini et al., 2012):

- Four bands at 10 m: the classical blue (490 nm), green (560 nm), red (665 nm) and near-infrared (842 nm).

- Six bands at 20 m: four narrow bands in the vegetation red-edge spectral domain (705 nm, 740 nm, 783 nm and 865 nm) and two large SWIR bands (1610 nm and 2190 nm).
- Three bands at 60 m: which are mainly dedicated to atmospheric corrections and cloud screening (443 nm for aerosol retrieval, 945 nm for water vapour retrieval and 1375 nm for cirrus cloud detection).

The mission foresees a series of satellites, each with a life time of 7.25 years, over a 20-year period. During full operation, two identical satellites will be maintained in the same orbit with a phase delay of 180°, providing a revisit time of five days at the equator. The first satellite, Sentinel-2A, launched in late 2013, and Sentinel-2B, about two years later.

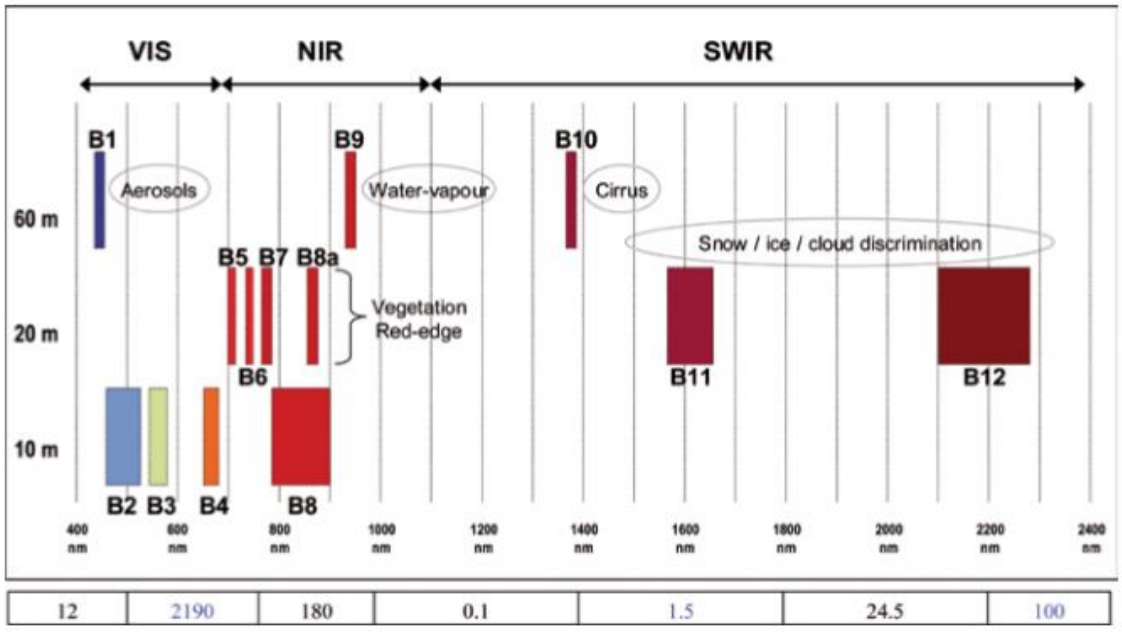

Figure (3.1); Spectral bands versus spatial resolution

3.1.2 Software

The following software have been utilized during the course of the present study:

- ENVI 4.8. and Arc GIS 10.2, for digital image processing and GIS manipulations.

- Microsoft Word, Excel 2010, for word processing and calculations.
- Global mapper, for changing DEM data format
- Gravmodel, for quantitative analysis of gravity data.

3.2 Methods

The methodology adopted in the present work involves digital image processing of remotely sensed data which is directed towards the enhancement and image transformation procedures in order to increase the visual interpretability and produce images suitable for geological interpretation.

Different processing techniques were utilized such as color compositing, band rationing, spatial resolution enhancement, principal component analysis (PCA), filtering and decorrelation stretching. The enhanced images were all imported into the GIS environment for delineation of geological boundaries and structures, together with the joint analysis and interpretation which facilitated the production of the geological map of the study area.

The gravity data in the form of free air anomaly was used to calculate the Bouguer anomaly. The computed Bouguer anomaly data were export into the ArcGIS to product Bouguer anomaly map. The regional and residual components of the gravity field were separated making use of the weighted average method. Afterwards, both the regional and residual gravity anomaly data were exported into ArcGIS for the data interpolation and production of the regional and residual anomaly maps. In order to investigate the subsurface structures, two gravity profiles are constructed cutting the most prominent anomalies in the area. The residual gravity anomaly along the profiles was used to produce 2.5 model. The flow chart of the adopted methodology is presented in Figure (3.2).

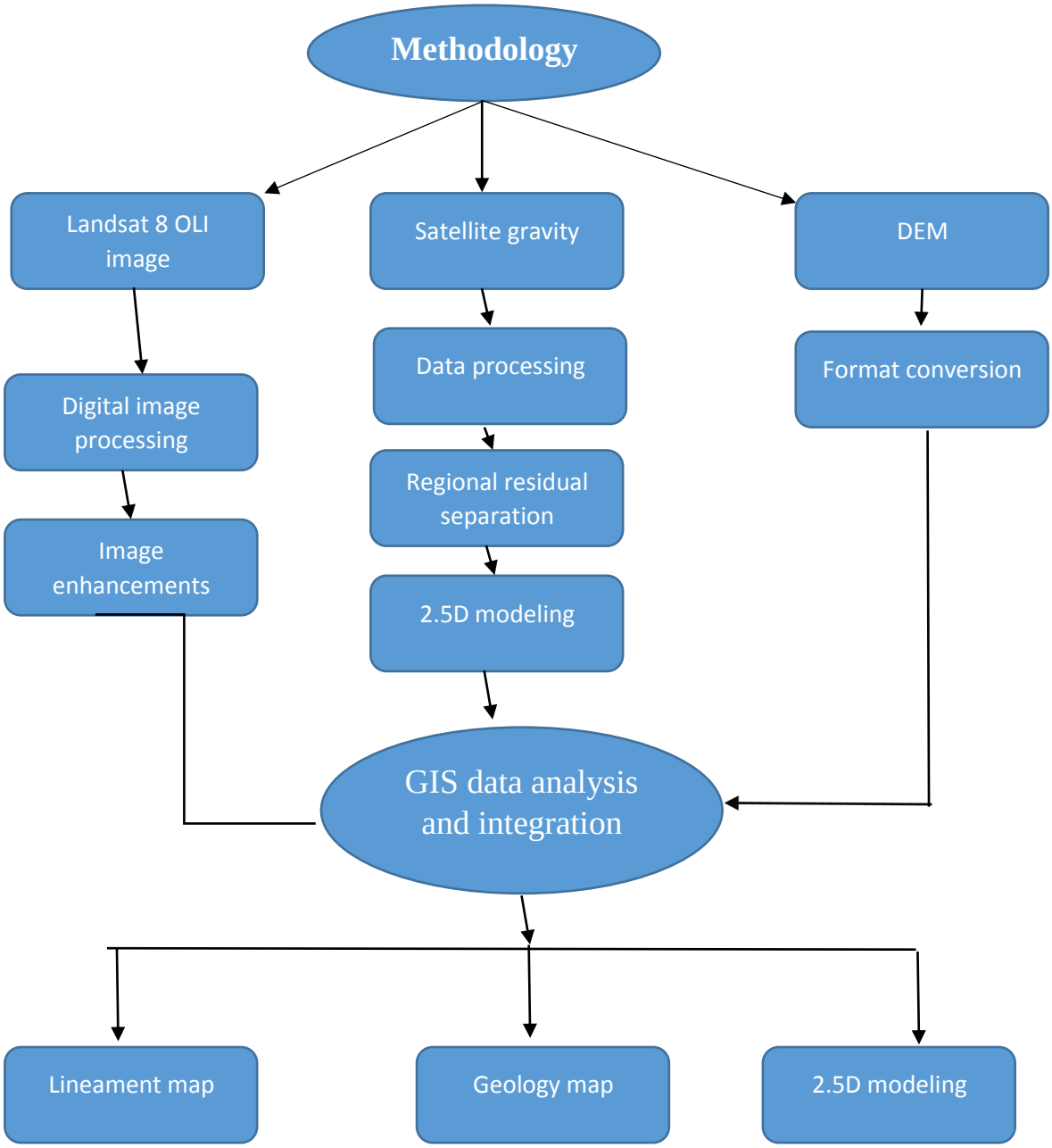

Figure (3.2): Flow chart of the methodology adopted in the present study

CHAPTER FOUR: REMOTE SENSING AND GEOPHYSICAL INVESTIGATIONS

4.1 Introduction

Remote Sensing is the science and art of obtaining information about an object, area, or certain phenomena through the analysis of data acquired by a device that is not in contact with the object, area, or phenomena under investigation. Normally, this gives rise to some form of imagery which is further processed and interpreted to produce useful data for application in agriculture, forestry, geography, geology and some other fields (Lillesand et al., 2003).

The primary objective of remote sensing is to extract environmental and natural resource data related to the earth (Lo, 1995). In remote sensing, the sun is the most obvious source of Electromagnetic Radiation (EMR), although all terrestrial objects are also sources.

atmospheric scattering is the unpredictable diffusion of radiation by particles in the atmosphere. There are three types of scattering, the first is Rayleigh scatter, which is common when radiation interacts with atmospheric molecules and other tiny particles that are much smaller in diameter than the wavelength of the interacting radiation. The second is Mie scatter, which exists when atmospheric particle diameters essentially equal the energy wavelengths being sensed. Water vapor and dust are major causes of Mie scatter. The last is non-selective scattering, which is non-selective in respect to the wavelength, i.e. all wavelengths of light are scattered, not just blue, green, or red (Lillesand and Kiefer 1999)

In contrast to scatter, atmospheric absorption results in the effective loss of energy to the atmospheric constituents. This normally involves absorption of energy at given wavelengths. The most efficient absorbers of solar radiation in this regard are water vapor, carbon dioxide, and ozone (O_3). Because these gasses tend to absorb electromagnetic energy in specific wavelength bands,

they strongly influence spectrally with any given remote sensing system (Lillesand et al., 2003) .

The earth surface is illuminated by solar energy. The reflected solar energy from the earth surface or the emitted electromagnetic energy by the earth surface itself is received by the sensor. The sensors are popularly known by the EMR region they sense. Remote sensing can be broadly classified as optical and microwave (Navalgund et al., 2007).

Remote sensing and its products were used extensively during the course of the present study to discriminate the rocks units and delineate their boundaries. Moreover, it was utilized to delineate and analyze the structural features in the study area. Many outputs have been used as base maps in the production of the geological, structural, and drainage maps of the area. More details about the different uses of remote sensing are provided in the respective section of this dissertation.

4.2 Geological mapping

The first part of study involves the geological mapping, whereby the most exposed geological units were delineated. This involved the utilization of various digital image processing techniques aiming at enhancing the quality of the images for improved geological interpretation and mapping.

Image processing methods are designed to transform multispectral image data format into an image display that either increases contrast between interesting targets and the background or yields information about the composition of certain pixels in the image (Kujjo, 2010).

Digital processing and analysis is more recent with the advent of digital recording of remote sensing data and the development of computers. Both manual and digital techniques for interpretation of remote sensing data have their respective advantages and disadvantages. The exact characteristics useful

for any specific task and the manner in which they are considered depend on the field of application. However, most applications consider the following basic characteristics, or variations of them: shape, size, pattern, tone (or hue), texture, shadows, site, association, and resolution (Olson, 1960). The utilized digital image procedures are described briefly in the following sections:

4.2.1 Creation of Meta file

A meta-file was created using Landsat 8 OLI bands of 30-meter spatial resolution. This file contains bands including visible (band 2, 3 and 4), near-Infrared (band 5) and Shortwave infrared (band 6 and 7). In addition to this metafile, an individual file of the panchromatic band 8 of 10-m spatial resolution. was treated separately and used in further processing to be combined with the multispectral data sets.

4.2.2 Image subset

Image sub-setting was used to resize the image data to cover only the study area in order to reduce the size of the dataset and speed the processing. In the present study in order to ease the subsequent digital images processing, spatial subset was created for both of the metafile and the panchromatic band in order to spatially resize the image to the following coordinate: long.: 32°35′00″ 32°46′00″ E and lat.: 16°13′00″ - 16°22′00″N.

4.2.3 Spatial resolution enhancement

CN Spectral sharpening tool is an extension of the Color Normalized algorithm often used to pan sharpening three-band RGB image. CN spectral sharpening to simultaneously sharpen any number of bands and retain the input image's original data type and dynamic range (ENVI, 2010).

CN Spectral Sharpening's algorithm, also referred to as the Energy Subdivision Transform, uses the higher spatial resolution (and lower spectral resolution) bands from a sharpening image to enhance the lower spatial resolution (but

higher spectral resolution) bands of the input image ENVI sharpen input bands only if they fall within the spectral range of one of the sharpening image's bands; all other input bands are unchanged in the output. The spectral range of the sharpening bands are defined by the band center wavelength and full width-half maximum (FWHM) value, both obtained from the sharpening image's header file (ENVI, 2010).

In the present study for Sabaloka volcanic plateau, image sharpening technique was utilized to enhance the resolution of the multispectral OLI image, to make the feature clearer and obtain more reliable information related to this study. Accordingly, the image sharpening was used to automatically fuse a low-resolution (30 meter) multispectral bands of Landsat 8 OLI image with a high-resolution (10 meter) panchromatic band of Sentinel MSI (gray scale image) using Gram schemed fusion technique. The output RGB images will have the pixel size of the input high-resolution data (10 meter). Example images of the fused image are presented in Figures (4.1 and 4.2).

Figure (4.1): color composite image of Landsat 8 OLI bands 7,5,2 in RGB, respectively, with resolution 10 meter.

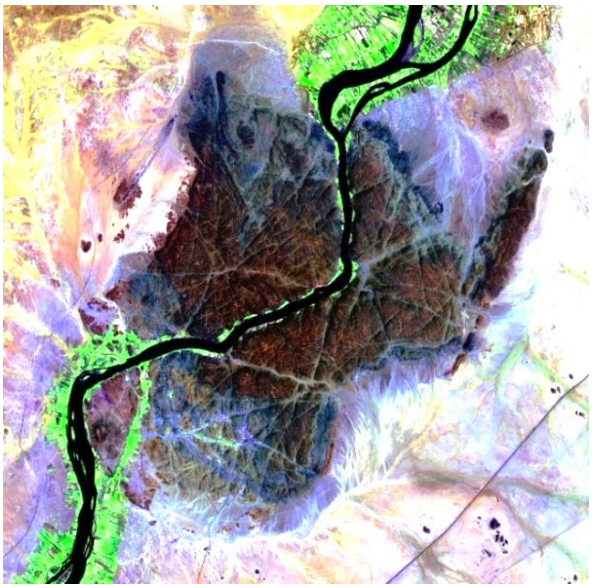

Figure (4.2): color composite image of Landsat 8 OLI bands 7,5,2 in RGB, respectively, have resolution 10 meter.

4.2.4 Color composite

The rule of color composites is to set the most informative band for a particular purpose in the red the next in green, and the least informative band in blue guns (Drury, 1993). Color photographs and images have certain advantages stemming from the fact that human eyes have better chromatic discrimination (Drury, 1993). Any three bands of six OLI multispectral bands can produce color composite image.

In the present study, the prepared color composites are exemplified by RGB, standard color composites that were created, namely: OLI 752 and 765 in RGB, respectively. Figures (4.3) and (4.5) show contrast-stretched color composite images of bands 7, 5, 2 and 7, 6, 5 in RGB, respectively. The creation of different (RGB) combinations was helped in the discriminate of the various rock types which is useful in delineating the geological boundaries.

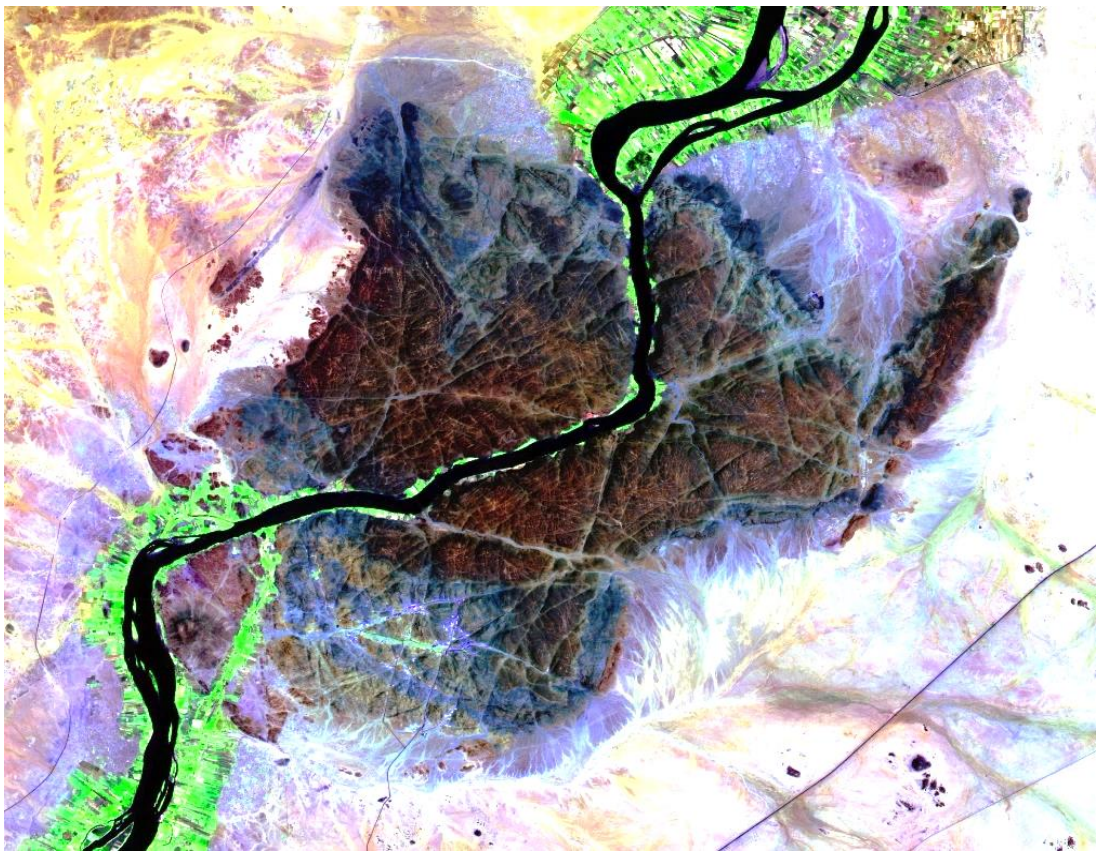

Figure (4.3): Color composite image of 8 OLI bands 7, 5, and 2 in R, G, and B, respectively.

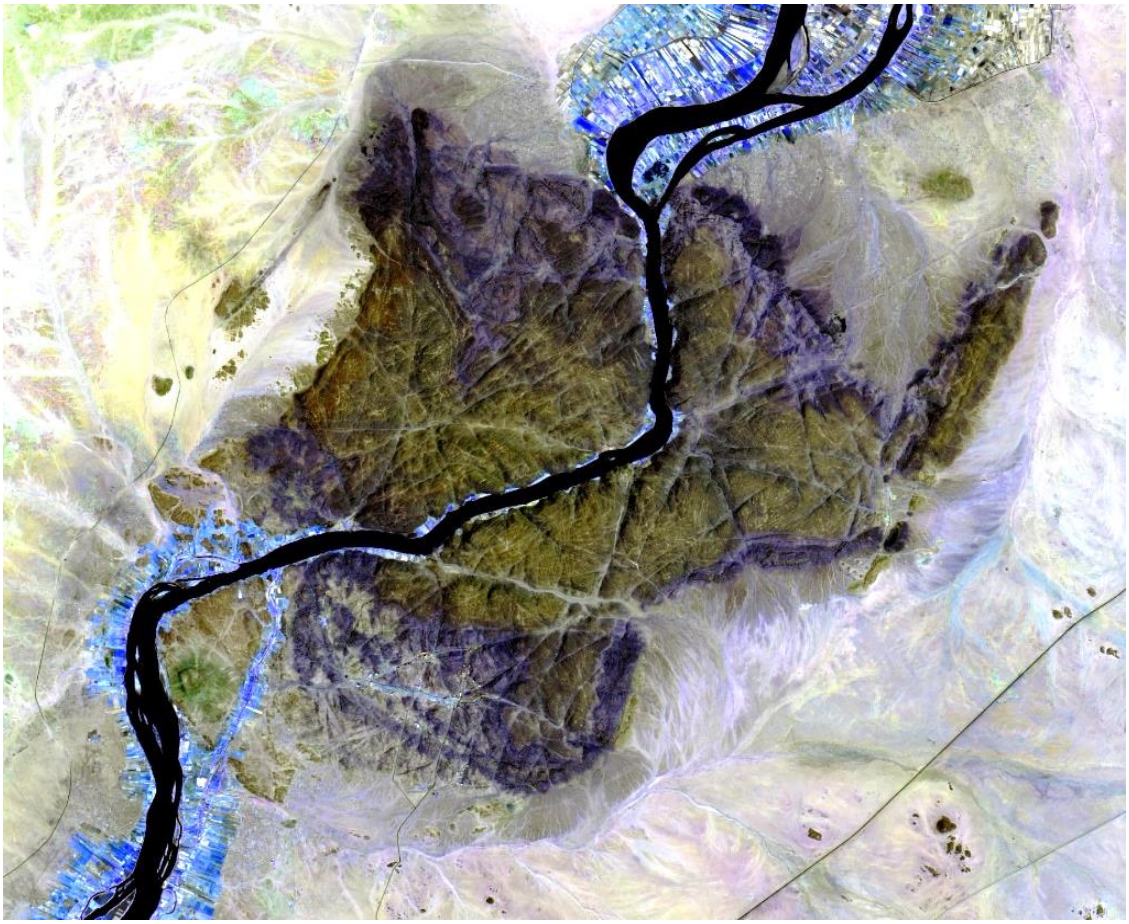

Figure (4.4): False color composite image of 8 OLI bands 7, 6, and 5 in R, G, and B, respectively.

It is clear from these images, as in Figure (4.3), that the area is volcanic plateau with isolated hills and peneplain which merges gradually with the River Nile flood plains. Whereas, the basement rocks show violet color related to the weathering products of metamorphic rocks, the volcanic plateau agglomerate and basalt show dark dray color, the dark and light ignimbrite show deep brown and verdurous brown huge, respectively. The Nile silt show green color, while the microgranite and syn- to late-orogenic granite shows brown color. The Cretaceous sediments show light brown color and the contact between basement rocks and Cretaceous sediments is clearly seen. The superficial deposits are displayed in yellow hues. The linear features are very clear.

4.2.5 Spectral band ratioing

Ratio images are known for enhancement of spectral contrasts among the bands considered in the rationing and have successfully been used in mapping alteration zones (Segal, 1983; Kenea, 1994).

Band ratios are used to enhance the spectral differences between bands and to reduce the effects of topography. Dividing one spectral band by another produces an image that provides relative band intensities. The image enhances the spectral differences between bands. Three ratios may be combined into a color-ratio -composite image to determine the approximate spectral shape for each pixel's spectrum (ENVI, 2010). Band ratio technique may also be applied to extract information not really seen in any single image (Gupta, 2003).

In the current study rationing and multiplication techniques were used following the general methodology of Sultan who noted that certain band ratios are particularly useful for lithological discrimination. Accordingly, ratio images were prepared during this study for the purpose of geological mapping. OLI bands ratios: 6/7, 6/2 and (4/5*6/5) in R, G and B, respectively were computed. The resulted image of this computation is presented in Figure (4.5).

It is clear from this image that the basement rocks appear in light to deep green and in some parts in cyan colors. The volcanic rock in the volcanic plateau and the tongue appear in deep blue; the syn- to late-orogenic granite appears in dark blue color, whereas the Cretaceous sandstone is displayed in pinkish color as in the case of J. Umm Marahik and Alrawyan. Nevertheless, the superficial deposit and the Nile silt are shown in orange color. The lineament features are very clean they contain sediments that appear in pinkish color.

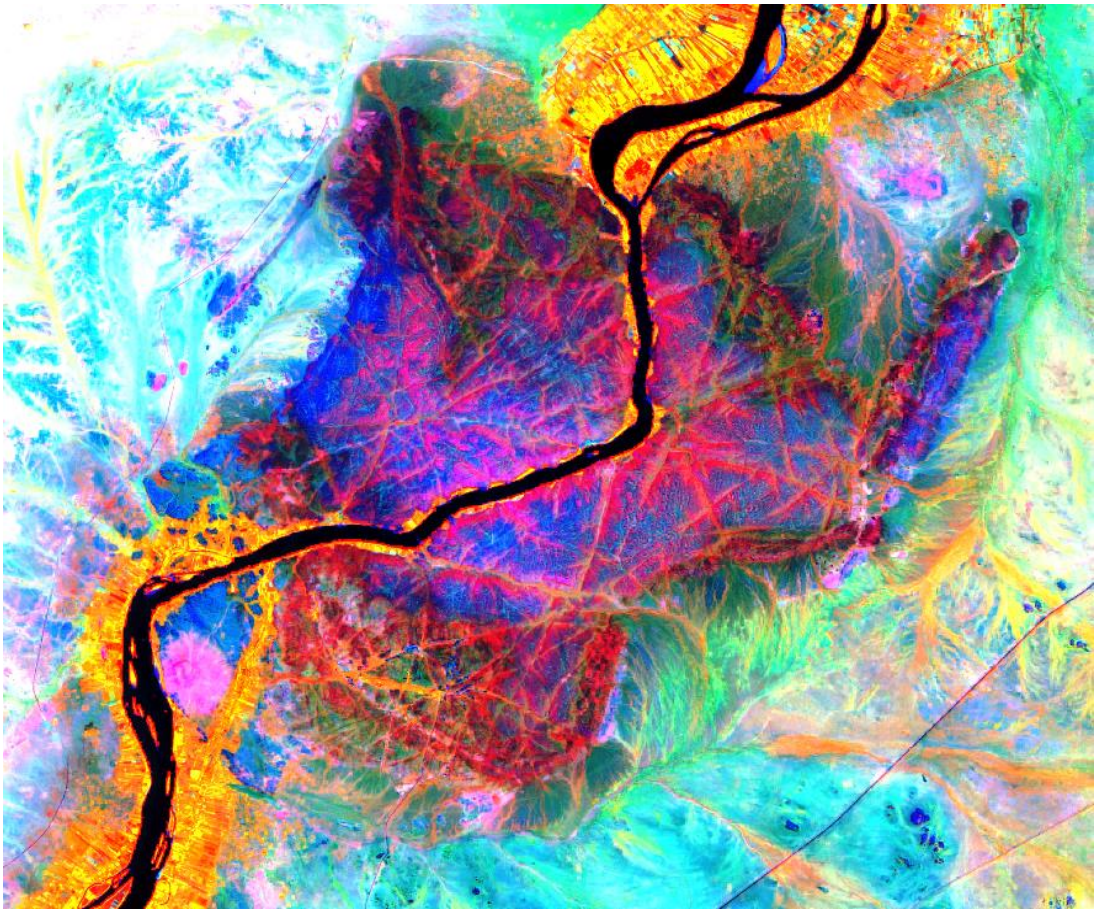

Figure (4.5): Color composite of Sultan ratio image of OLI bands 6/7, 6/2, and 6/5*4/5 in R, G, and B, respectively.

4.2.6 Principal Component Analysis (PCA)

Principal Component Analysis Originally known as the Karhunen- Loeve transformation is used to compress multi-spectral data sets by calculating a new coordinate system. The method represents a powerful means of Suppressing irradiance effects that dominate all bands so that geologically interesting spectral reflectance features of surface materials can be examined (Sabins, 1999). The PCA is a multivariate statistical technique used to decrease the data-redundancy of the correlated image that has much higher contrast than the original bands. The produced number of output PC bands is the same as the number of the input spectral bands (Vincent, 1997).

Principles components analysis comprise a linear stretching that deals with the statistics of the scene data to identify the rotation of the original data axes by computing a new orthogonal coordinates system that point in the direction of

decreasing order of variances (Elkhound and Singh, 1993). For each pixel, new DNs are determined relative to each of the new coordinate's axes. The first three PC images contain 97 percent of the variation of the original six bands, which is an important compression of data. The PCT increases overall separbility and reduces the dimensionality and for thus it's highly useful in the image classification (Gupta, 2003).

The first PC band contains the largest percentage of data variance and the second PC band contains the second largest data variance, and so on. The last PC bands appear noisy because they contain very little variance, much of which is due to noise in the original spectral data. principal components bands produce more colorful color composite images than spectral color composite images because the data is uncorrelated (ENVI, 2010).

The computed PCs of the current study are presented in Figures (4.6). It can be seen that the PC1 and PC2 display more lithological contrast, and the topographic expression is better and it is known that they discriminate well between the VNIR and SWIR bands. Both PC3 and PC4 although they have low variance value but still display fair lithological contrast, whereas the rest PC5 and PC6 with very low variance, are less informative and show only noise.

4.2.7 Decorrelation Stretching

The decorrelation stretching is use to remove the high correlation commonly found in multispectral data sets and to produce a more colorful color composite image. The highly correlated data sets often produce quite bland color images. Decorrelation Stretching requires three bands for input. These bands should be stretched byte data or may be selected from an open color display (ENVI, 2010).

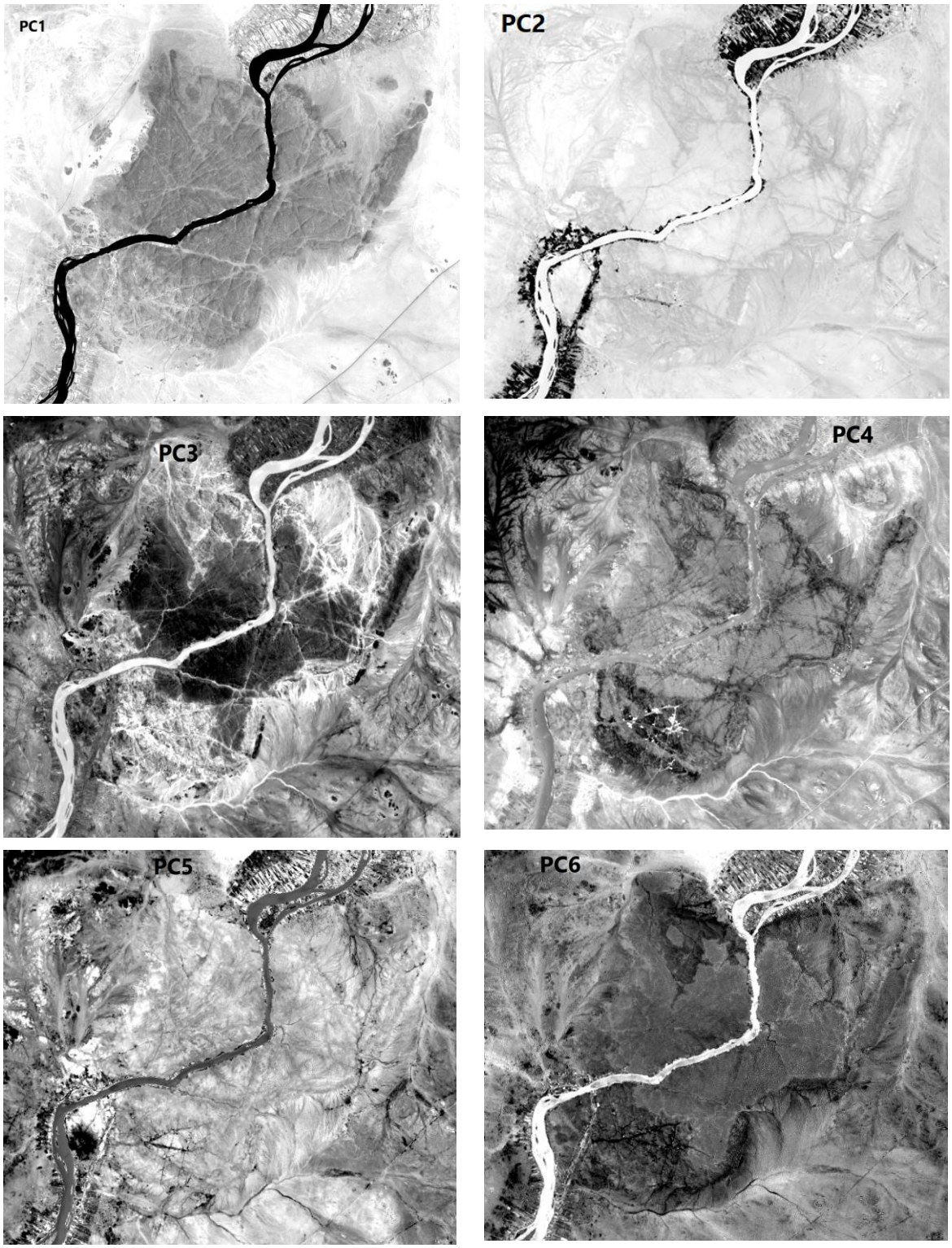

Figure (4.6): PC1, PC2, PC3, PC4, PC5 and PC6 displayed in the grey scale.

Decorrelation stretching enhances the color separation of an image of highly correlated bands. The exaggerated colors improve visual interpretation and make feature discrimination easier. This technique originated as an adaptation

and extension of closely related data transformation technique of the principal component transformation (Dasu et al., 2011).

In this context, the decorrelation stretching technique has been applied on two sets of colored composite images of bands (7, 5, 2) and (7, 6, 5) presented in Figures (4.7 and 4.8), respectively. The two images show more saturated hues than the normal linear stretched ones. The decorrelation stretched image of bands 7,6,5 in Figure (4.7) is better in revealing the differences between various lithological units and salient structural elements than that of the decorrelation stretched image of bands 7, 5, 2 of Figure (4.8).

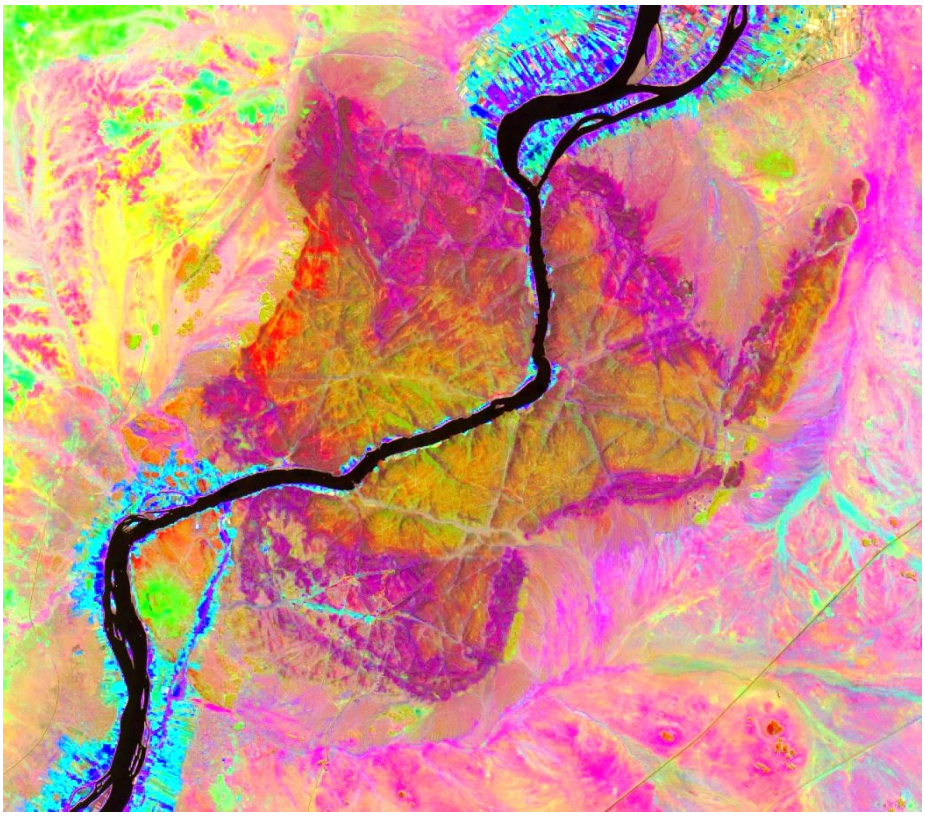

Figure (4.7): Decorrelation stretched color composite image of Landsat 8 OLI bands 7, 6, 5 in R, G, and B, respectively

In the above image, the basement rocks are shown in light brown and pinkish colors, the agglomerate appears in dark purple color, the light ignimbrite is shown in light purple color, whereas the dark ignimbrite is portrayed in golden yellow. The Cretaceous sandstone appears in green, the superficial in yellow and the Nile silt in cyan and blue colors. The lineament features are clear.

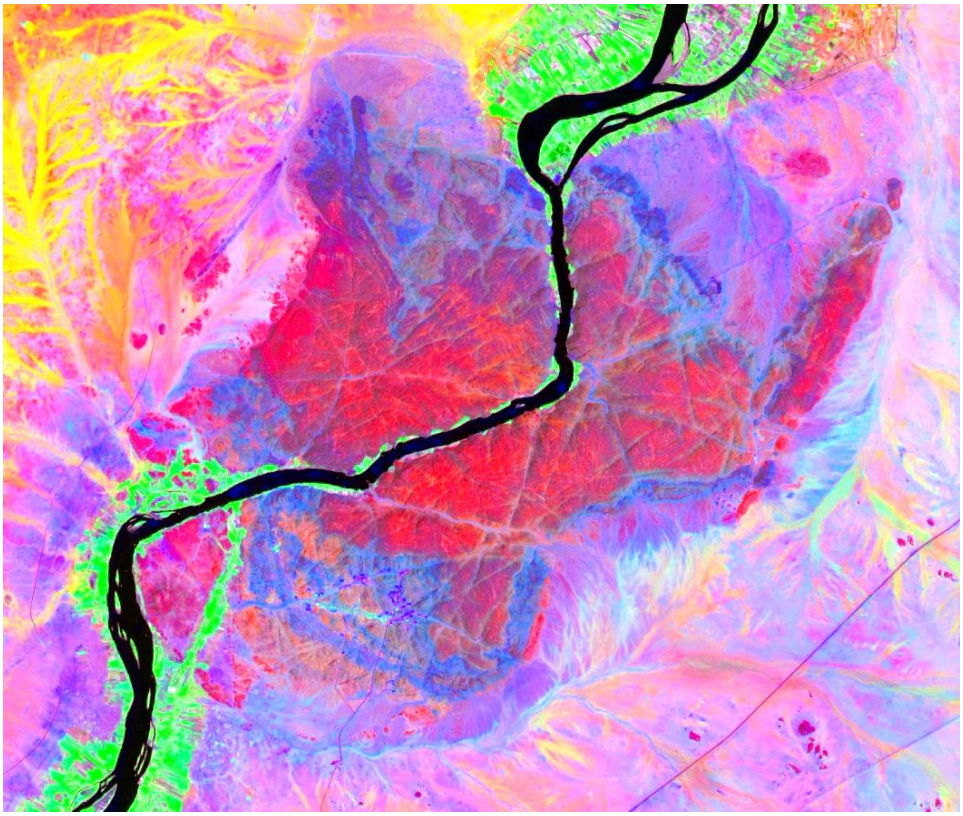

Figure (4.8): Decorrelation stretched color composite image of Landsat 8 OLI bands 7, 5, 2 in R, G, and B, respectively.

In the image provided in Figure (4.8), the delineation of the ridges is very difficult, this is because the blue color is very common in the image and many rock types are displayed in the same color.

4.2.8 High pass filtering

Convolution filters produce output images in which the brightness value at a given pixel is a function of some weighted average of the brightness of the surrounding pixels. Convolution of a user-selected kernel with the image array returns a new, spatially filters image. By selecting the kernel size and values, different types of filters can be produced. Standard convolution filters include:

- **High Pass**: Removes the low frequency components of an image while retaining the high frequency (local variations). It can enhance edges between different regions as well as to sharpen an image. This is

accomplished using a kernel with a high central value, typically surrounded by negative weights.

- **Low Pass**: Preserves the low frequency components of an image, which smooths it (ENVI, 2010).

Filtering is a very important research field of digital image processing. all filtering algorithms involve neighborhood processing because they are based on the relationship between neighboring pixels rather than a single pixel in point operations. Digital filtering is useful for enhancing spatial features such as lineaments that may represent significant geological structures such as faults, veins or dykes. It can also enhance image texture for discrimination of lithology and drainage patterns (Liu and Mason, 2009).

In this study, the high spatial filtering was applied to enhance the linear feature present in the study area Figures (4.9 and 4.10).

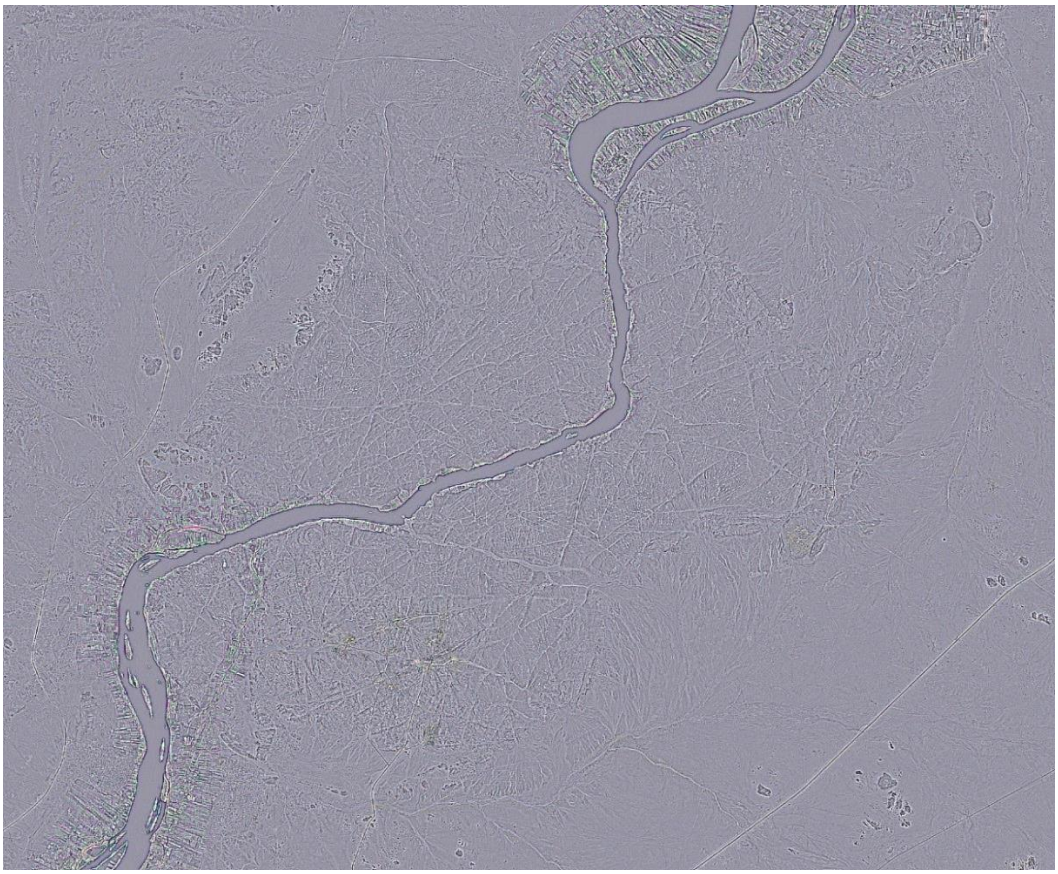

Figure (4.9): High pass filtering image for composite color of Landsat 8OLI bands 7, 5, 2 in R, G, and B, respectively.

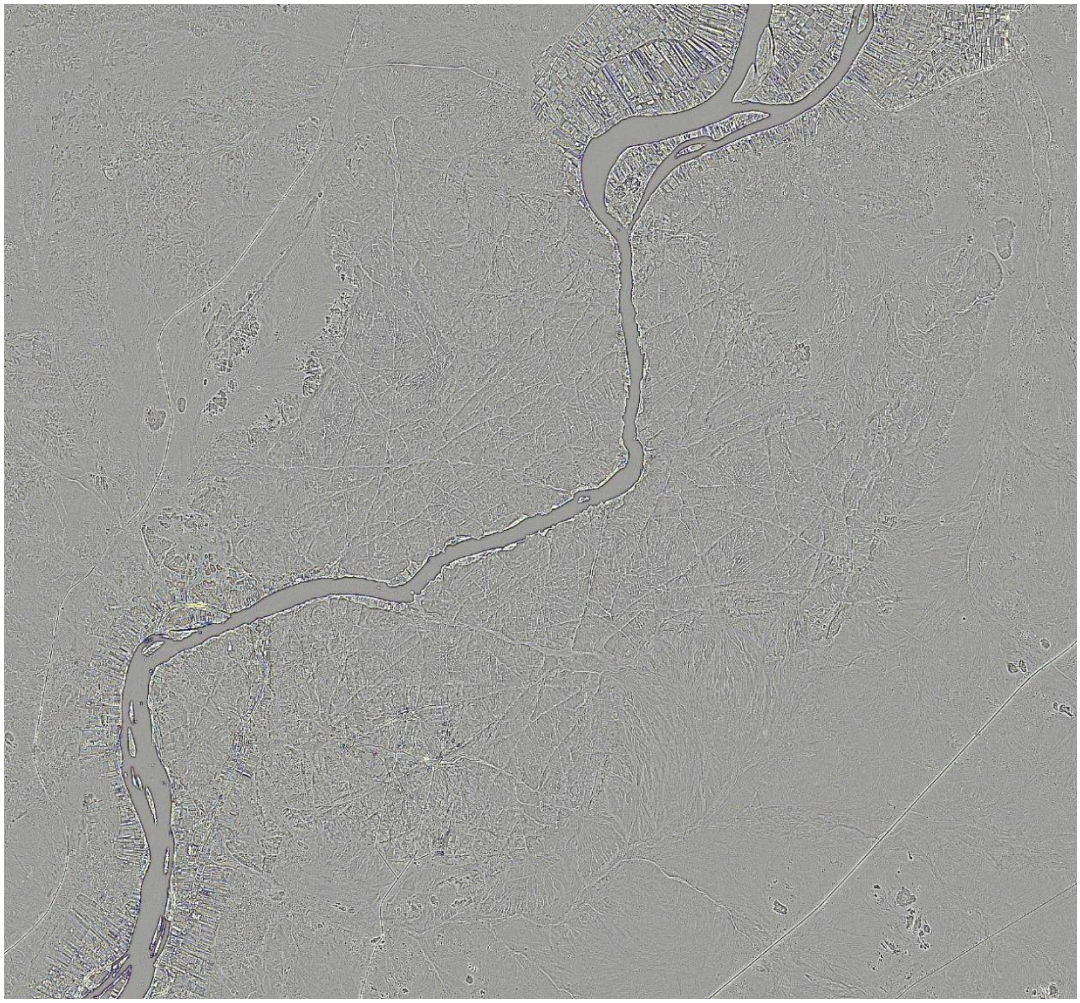

Figure (4.10): High pass filtering image for composite color of Landsat 8OLI bands 7,6, 5 in R, G, and B, respectively.

4.2.9 GIS data integration and analysis

Geological mapping has been increasingly supported by the use of remote sensing and GIS techniques, which improve the quality and timely availability of basic information for exploration activities *(List and Squares, 1996).* Based on their spectral signatures in different colour composite imageries, the discriminated lithological units represent the geological units of the map area. The Geo-database facilitate the use of the integrated various data as registered multi-layers.

GIS technology is increasingly being used in spatial decision support systems. A GIS system stores spatial data in a digital mapping of environment. A digital

base map can be overlain with data or other layers of information onto a map in order to view spatial information and relationships. The ability of GIS to integrate maps and data bases, using the geography as the common feature among them has been extremely effective in the context of planning development. the attribute data base can be analyses by multiple queries, linked to multiple databases related to different projects to arrive at a comprehensive picture of the current scenario in a given area (Keenan, 1997).

In the present study, the remote sensing OLI image analysis; the different color composite imageries, PC spectrally sharpened image, decorrelation stretched image, and sultan ratio color composite image were imported into Arc GIS 10.2. This software was actually the platform where the delineation of the boundary between the different lithological units was conducted. Moreover, the delineation of linear structures present in the Sabaloka Igneous Complex and drainage maps were also carried out.

4.2.9.1 Lithological discrimination

GIS based, on screen digitization has been used to draw the boundaries of the various lithological units. This process facilitated the production of a lithological map.

4.2.9.2 Linear structures mapping

The term lineaments have been used in the literature to elect different meanings. It has been applied to orientation of natural as well as man-made features. In the geology field lineaments indicate shear zones; fold axial traces, joints, fractures, faults, dykes, streams or layering. Terrain-related lineaments might occur as straight, curvilinear, parallel or en-echelon patterns and are generally related to fracture systems, discontinuity planes, fault traces and shear zones, the manifestation of the lineaments is dependent on the scale of the observation and dimensions involved (Gupta, 2003). The structural analysis of lineaments

is an important step in acquiring a basic knowledge about the structural evolution of an area.

in the present study a Gram-Schmidt pan-sharpen image together with the spatially filtered images have been used within the GIS, where on screen digitization has been conducted to draw a number of about 225 lineaments that range in length from 544 m to 2310m (Figure 4.11).

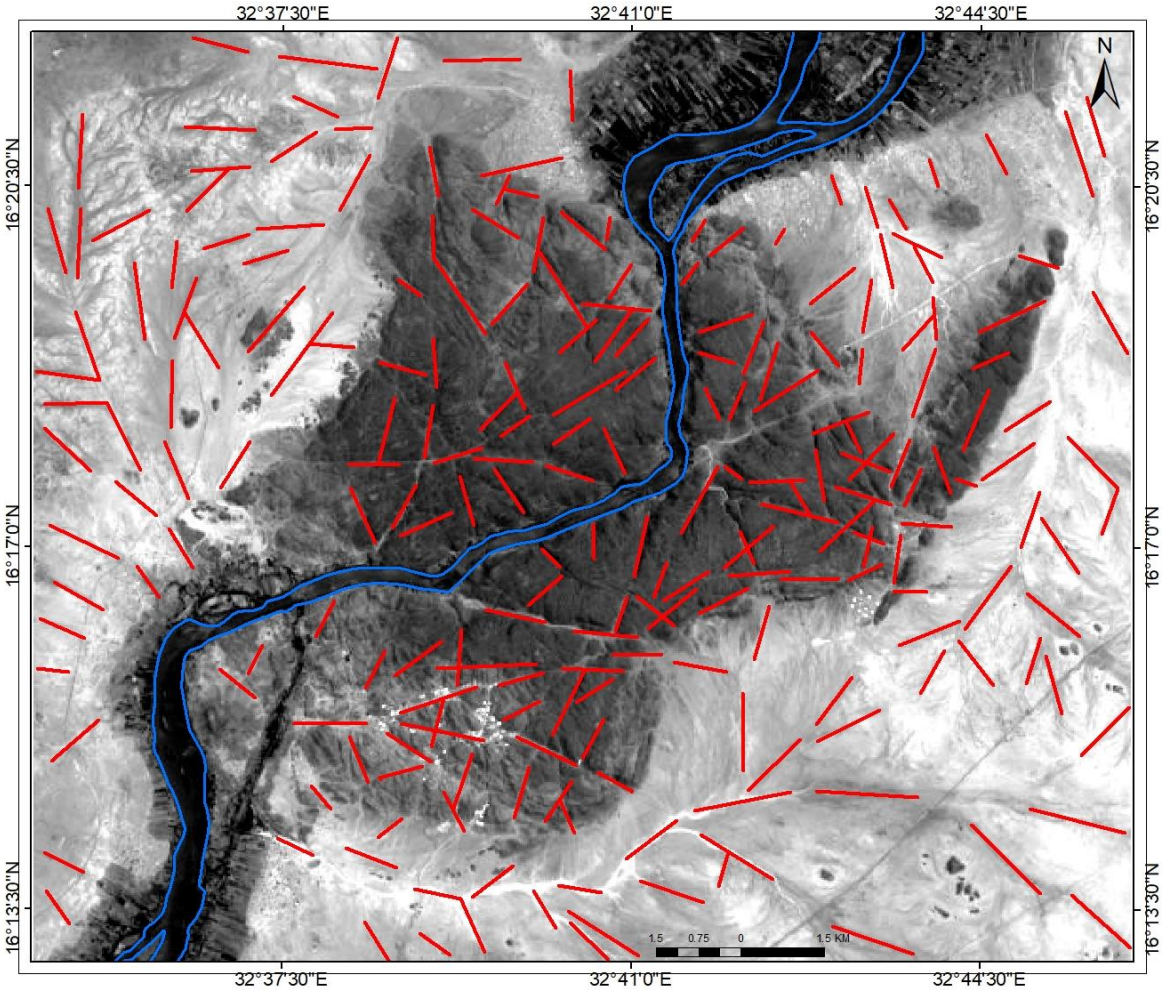

Figure (4.11): Lineament map of Sabaloka Igneous Complex

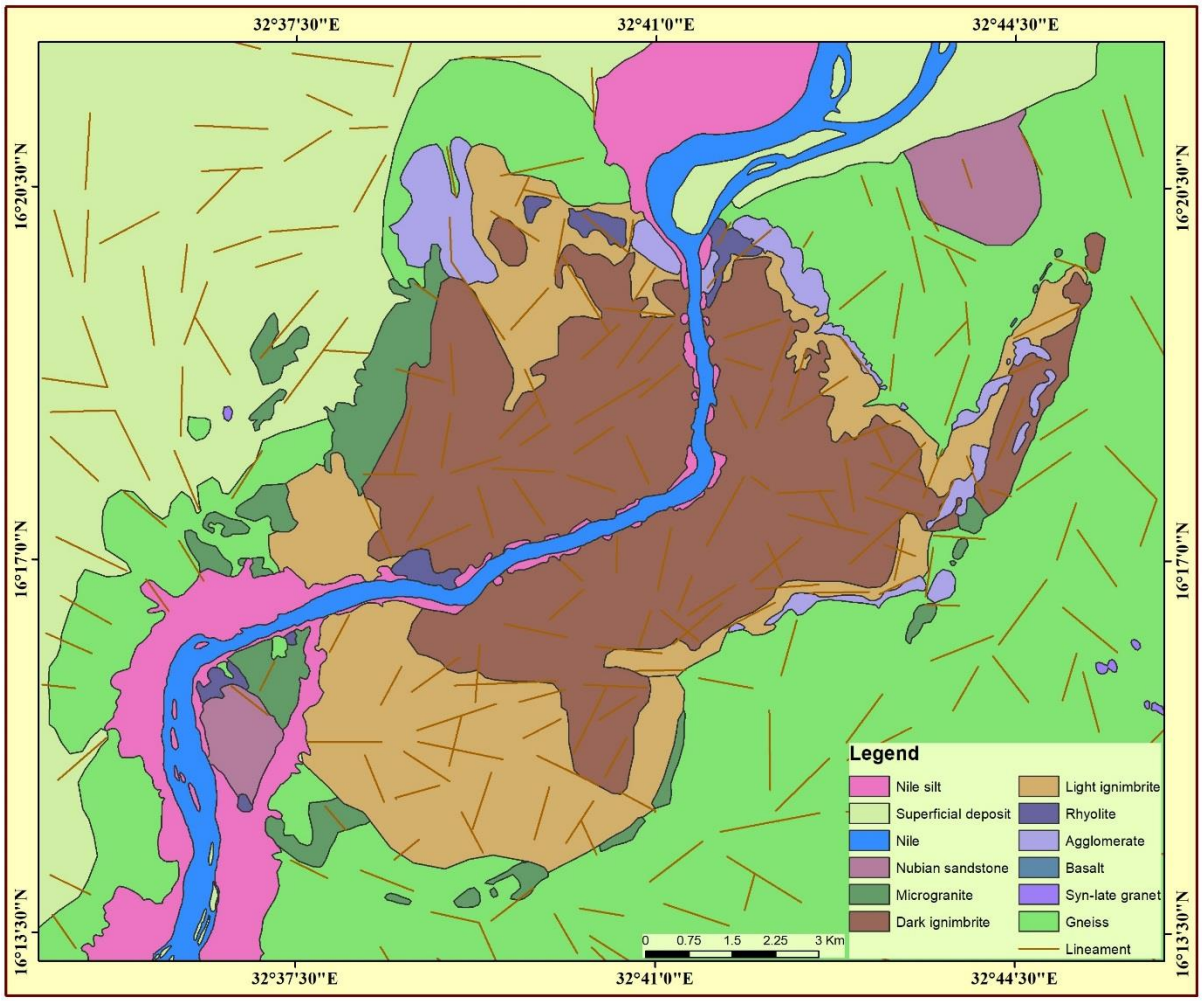

Figure (4.12): Geological map of Sabaloka Igneous Complex.

Most outcrops of rocks exhibit many fracture that show very small or unobservable displacement normal to their surface, not all fracture in volcanic rock are tectonic origin they are mainly cooling joints whereby there are some fracture related to the post cretaceous local faulting like Umm Maraheik fault. Also the derailing system in the area show in lineament phenomena.

From the geological map (Figure 4.12), it can be seen that the area forms an inlier that consist of different type of rocks ranging from metamorphic (gneiss and migmatites) through igneous (Sabaloka Igneous Complex; Plate 4.1) and basaltic lava, rhyolite, agglomerate, ignimbrite and microgranite (Plate 4.2) to sedimentary (Cretaceous sandstone).

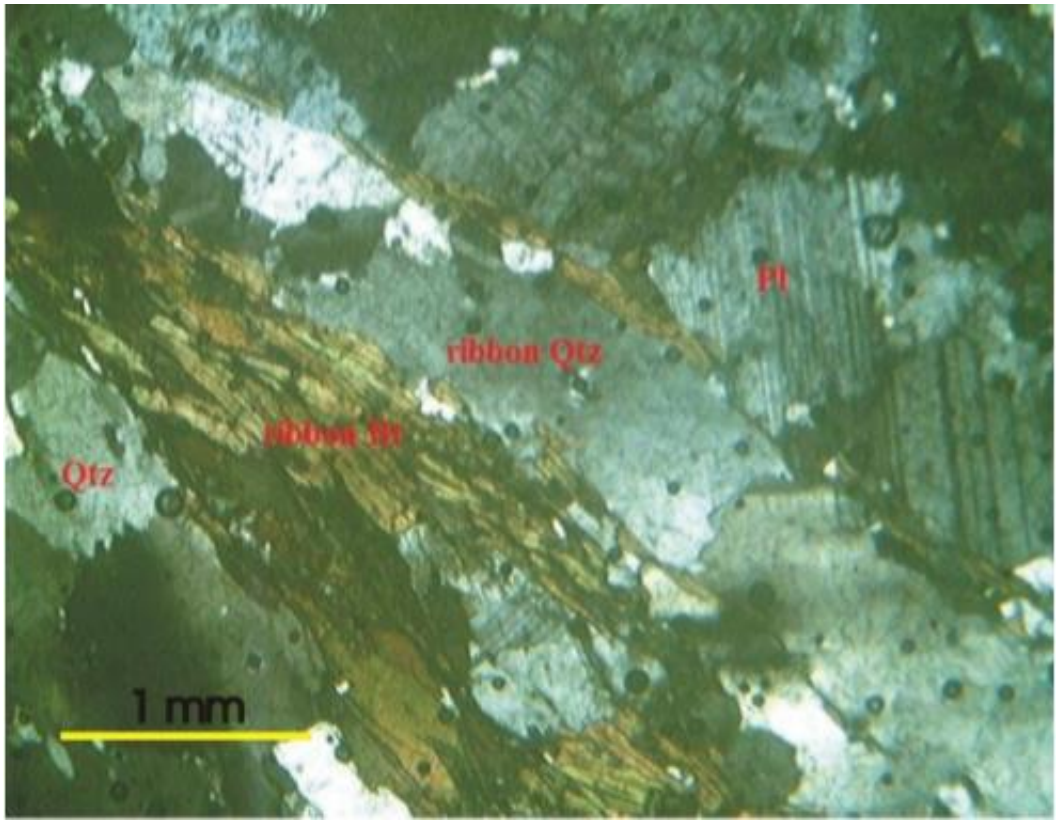

Plate (4.1): Microscopic view of biotite gneiss rocks (XPL view). Note: Qtz= Quartz, Pl= Plagioclase, and Bio= Biotite.

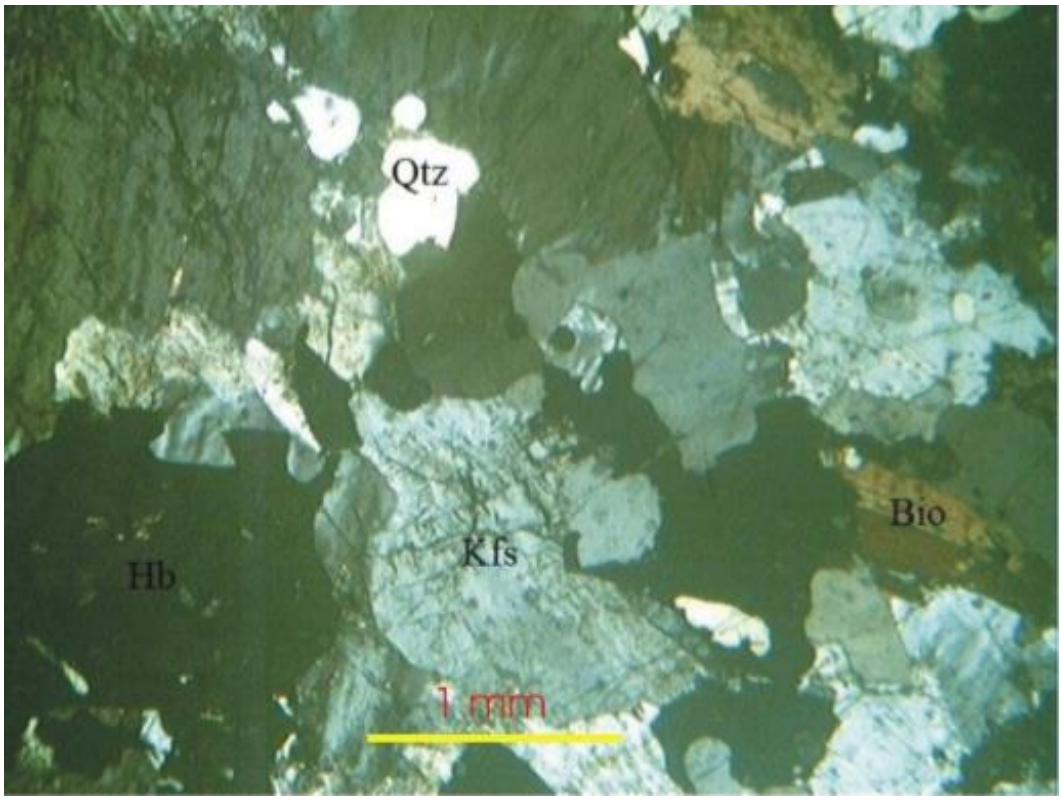

Plate (4.2): Microscopic view of granite Rock. Note: Kfs = k-feldspar, Hb = hornblende.

4.3 Gravity Investigations

4.3.1 Introduction

The gravity method is a non-destructive geophysical technique that measures differences in the earths' gravitational field at specific locations. It has found numerous applications in engineering, environmental and geothermal studies including locating voids, faults, buried stream valleys, water table levels and geothermal heat sources. The gravity method depends on the bulk density so the differing in gravitation field due to different earth materials have different bulk density .

These variations can then be interpreted by a variety of analytical and computers methods to determine the depth, geometry and density that causes the gravity field variations. The data are processed to remove all these predictable effects. The most commonly used processed data are known as Bouguer gravity anomalies, measured in mGal. A gravity meter or gravimeter measures the variations in the earth's gravitational field, the gravimeters have to be very sensitive so as to measure one part in 100 million of the earth's gravity field (980 gals or 980,000 mgals) in units of mgals or microgals .

Anomalies in the earth's gravitational field result from lateral variations in the density of subsurface materials and the distance to these bodies from the measuring equipment (Figure 4.13).

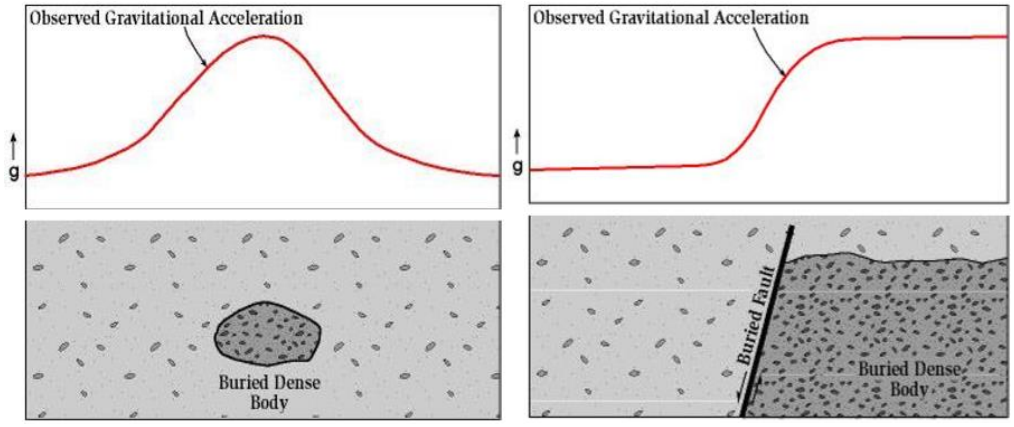

Figure (4.13): Illustrations showing the relative surface variation of Earth's gravitational acceleration over geologic structures.

DESCRIPTION OF ROCKS IN THE REGION

1. Basalt:

Mineral composition plagioclase, pyroxen and amphibole. Also, the texture fine, structure is massive, it is type of rocks igneous /basic and the color melano-critic.

2. AGLOMARITE TUFFS:

It is a fissile rock consisting of an acidic acid, a collection of pieces of glass and crystals that formed in addition to a fraction of the lava that previously cooled (basalt, rhyolite). These rocks are located above the lower roulette rocks in the rocky sequence of the Calderon complex.

3. AGENEMBRITETUFFS:

These rocks formed from the sedimentation and integration of volcanic ash, pyroclestic rocks formed from acidic and sometimes average fumes (Almond and Farouk 1993). These rocks contain glass shard, and pumice fragments, as well as rock fragments (basalt, roulette).

These rocks occupy the peak of the rock sequence for the volcanic plateau and the Acantbright rocks, some of which are light colored and others dark. This difference occurs in color due to the proportion of silica which increases in the lighter types and the glass fracture, which is the softest in the dark types.

The importance of the geothermal rocks in determining the end of volcanic activities (Nabil Mustafa Hafez et al. 1988) is the latest volcanic event on the plateau.

4. DARK AGENEMBRITETUFFS:

هو الذي يمتاز بالقطع الزجاجية الناعمة الي تعطيه اللون الداكن المميز له.

Mineral composition:

Quartz, feldspar, texture Utaxetic, type of rock igneous, mode of occurrence volcanic and clan acid.

1BIOTITE GNISSROCK

It is a mutant, grayish rock consisting of quartz, felspar, mica and granite.

Characterized by tawarruq in the rock

mile 30°
strike 180

5. MICRO GRANITEROCK:

The ring dyke was the result of the graben that occurred after the exit of the glamor and its accumulation above the magma chamber, thus forming a cauldron, resulting in the breakthroughs of the ring dyke group, which were extended in two separate sections by the foundation rocks, forming a ring chain that surrounds the rocks of the calderon complex (Almond and Farouk 1993).

This ring dyke is made up of Granit's granule and due to the descent process and changing conditions of the hardening of the granular magma, it is composed of porphyritic microgranite rocks.

- Flesite dykes and sheets.

The light-colored dykes are the fabric of its metallic composition of quartz quartz and feldspar feldspar and are made up of rouliate installation. Many of these cuttings are scattered on the southern edge of Calderon and near Mount Um Marahik.

6. اللسان البركاني:

الذي يكون حيّد برتفع عشرات الأمتار فوق سهل المحيط وتتبع له الجبيلات الحمر.

7. A MOUNT UM MRAHIK

The oldest rock is the gnayes and there is the mountain top of these rocks, and its relationship is uncomformaty, and consists mostly of sedimentary rocks with the difference of constituent minerals and matter and the rock is determined by the size of granules

8. الهضبة البركانية (plateau):

هي توجد فوق الفوهة البركانية، وتشمل جل التتبع تقريبا، وترتفع حوالي (450-500) متر فوق مستوى فوق سطح البحر، بمساحة 50 متر مربع، بحجم كلي حوالي 100 متر مكعب، وهي تكون ربوات عند حوافها، وترتفع هذه الربوات حوالي (50-100) فوق سطح المحيط.

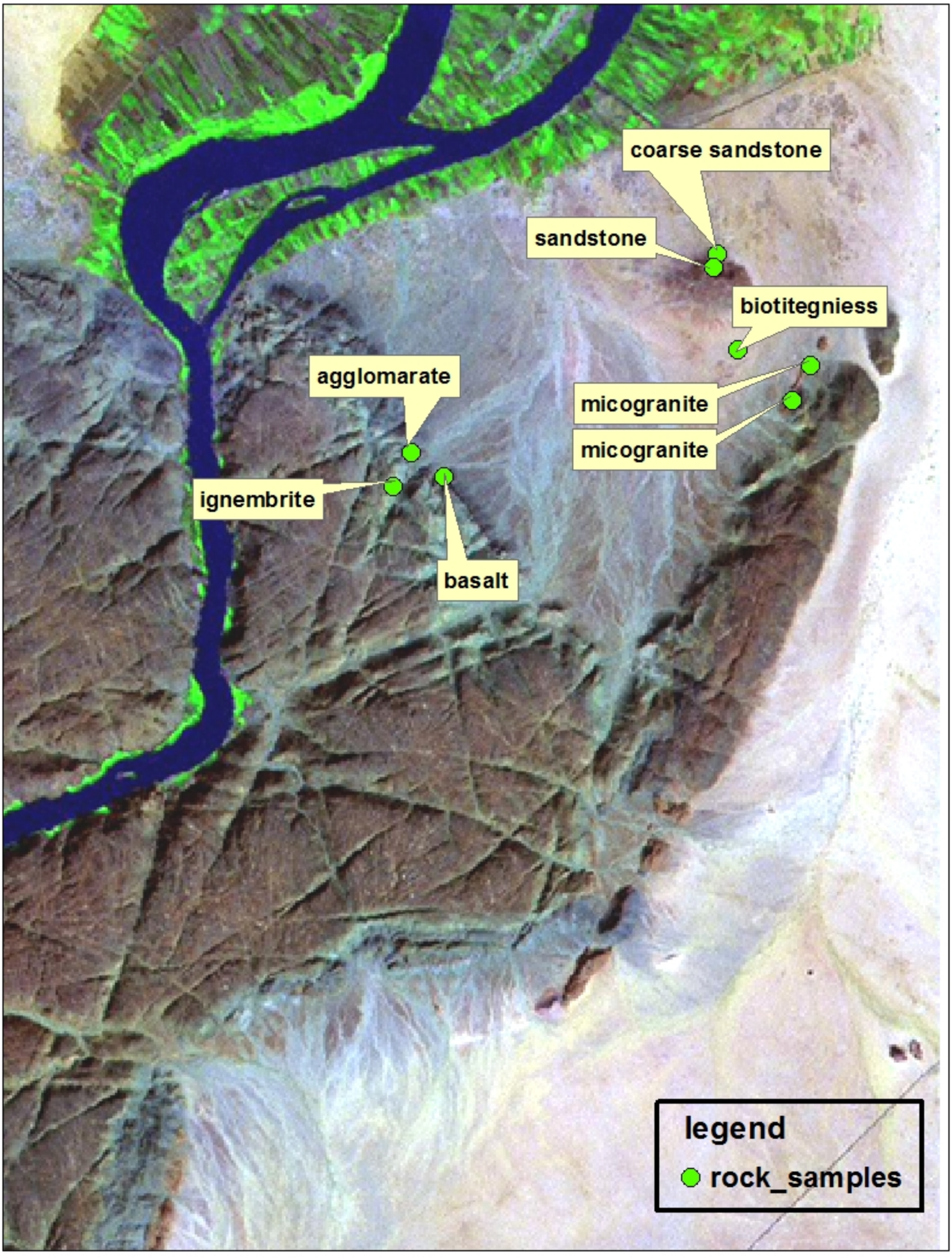
coarse sandstone
sandstone
biotitegniess
agglomarate
micogranite
micogranite
ignembrite
basalt
legend
rock_samples

4.3.2 Basic concept

The subsurface geology is revealed the interpreting gravity data that reflects the variation in earth gravitation field generated by density of rock unit that is different from surrounding. An accusative body represents a subsurface region of anomalous mass and causes localized perturbation in gravitation field known as gravity anomaly.

Avery wide range of geological situation gives rise to zone of anomalous mass that produces significant gravity anomalous. On the larger scale, granite plutonic and sedimentary basins generate major gravity anomalous .

The gravity survey theory basis in newton's low of gravitation, which states that the force of attraction (F) between two masses m_1 and m_2, whose dimensions are small with respect to the distance (r) between them is given by

$$F=GMm/R^2 =mg$$

Thus, we usually see the law of gravitation written as shown where **F** is the force of attraction, **G** is the gravitational constant, and **r** is the distance between the two masses, $\mathbf{m_1}$ and $\mathbf{m_2}$**.**

When making measurements of the earth's gravity, we usually don't measure the gravitational force, **F**, rather; we measure the gravitational acceleration, **g**. The gravitational acceleration is the time rate of change of a body's speed under the influence of the gravitational force.

In addition to defining the law of mutual attraction between masses, Newton also defined the relationship between a force and acceleration. Newton's second law states that force is proportional to acceleration. The constant of proportionality is the mass of the object. Combining Newton's second law with his law of mutual attraction, the gravitational acceleration on the mass $\mathbf{m_2}$ can be shown to be equal to the mass of attracting object, $\mathbf{m_1}$, over the squared distance between the center of the two masses, **r**.

$$g = \frac{GM_1}{r^2}$$

4.3.3 Satellite gravity

The Radar altimeter measurements provided the scientific community with valuable information about the earth interior (Nabigian et al., 2005.). From this, the sea-surface topography from radar altimeter data was used to calculate the vertical component of the gravity field. This significantly helped in improving the knowledge of the earth's tectonic (Hwang et al., 1998; Sandwell and Smith, 1997). Consequently, the gravity field measurements were moved from only calculating the marine gravity field from radar altimeter measurements to measuring the global gravity field using new satellite missions. This step led to improving the quality of the available data and also improving our understanding of the overall earth tectonic history (e.g. Tapley and Kim, 2001).

Satellite gravity is gravity field measurements that were available recently in the last decade. Recent satellite missions were launched such as CHAMP in 2000, GRACE in 2002, and GOCE in 2009 to map the Earth's gravity field (Tapley and Kim, 2001; http://www.nasa.gov). The global coverage and the consistent data quality are the most significant advantages of the satellite gravity data (Nabigian at al., 2005).

4.3.4 Satellite Gravity Data Processing and Interpretation

The interpretation of Bouguer gravity anomalies ranges from just manually inspecting the grid or profiles for variations in the gravitational field to more complex methods that involves separating the gravity anomaly due to an object of interest from some sort of regional gravity techniques including weighted averaging and polynomial surface fitting. The interpretation of separated (residual) gravity anomalies commonly involves creating a model of the subsurface density variations to infer geological cross-section. These models can be determined using a variety of methods ranging from analytical solutions

due to simple geometries (e.g., sphere) to complex three dimensional computer models.

Sabaloka Igneous Complex of late Pre- Cambrian or Cambrian age consists of an elliptical ring dyke of porphyritic micro granite surrounding acid volcanic rocks in the southern half of the area and a basement composed mainly of biotite gneisses in the north. Sandstones of the Nubian formation locally overlie the igneous rocks and the basement. The various rock types have different densities. The density measurements for all the sedimentary formations (2.67gm/cc) and the basement rocks of the area (2.4 gm/cc). accordingly, there are variations in the Earth gravity field due to the density contrast.

4.3.4.1 Bouguer anomaly

The satellite gravity data in the present study is provided in the form of Free Air Anomaly (FAA) together with the elevation data. Also to determine the elevation changes in the area, the digital elevation model data (DEM) was processed in the Global mapper software and exported into GIS environment.

When one increases elevation on the Earth, it usually implies that there is an additional mass between the original level and the new level. this additional mass itself will exert a positive gravitational attraction, which acts to reduce the Free-Air (negative) gravity change. the Bouguer gravity effect Δg_B is calculated on the basis of the gravitational attraction of a horizontal slab, of infinite extent and of thickness equal to the elevation difference, in accord with Equation

$$\Delta g_B = +0.04192d\ mGal$$

Where **d** is the mean density of the slab in g/cm^3. For gravity measurements beneath the surface of the Earth. the Bouguer effect will be negative. And hence the Bouguer Anomaly for each point, in accord with Equation:

$$\mathbf{BA = FAA - BC}$$

The results of computations were imported into the GIS environment with the DEM image for interpolation, which finally resulted in the preparation of Bouguer anomaly map of the study area with counter interval of 2 mGal (Figure 4.14).

The area was divided into a grid of cells with the height and width of the cell is 3.1Km. The centers of cells represent the points of the profiles. The grid is formed from 13 columns and 12 rows, meaning we have 13 vertical profiles covering our study area, while the distance between the profiles is 3.1Km.

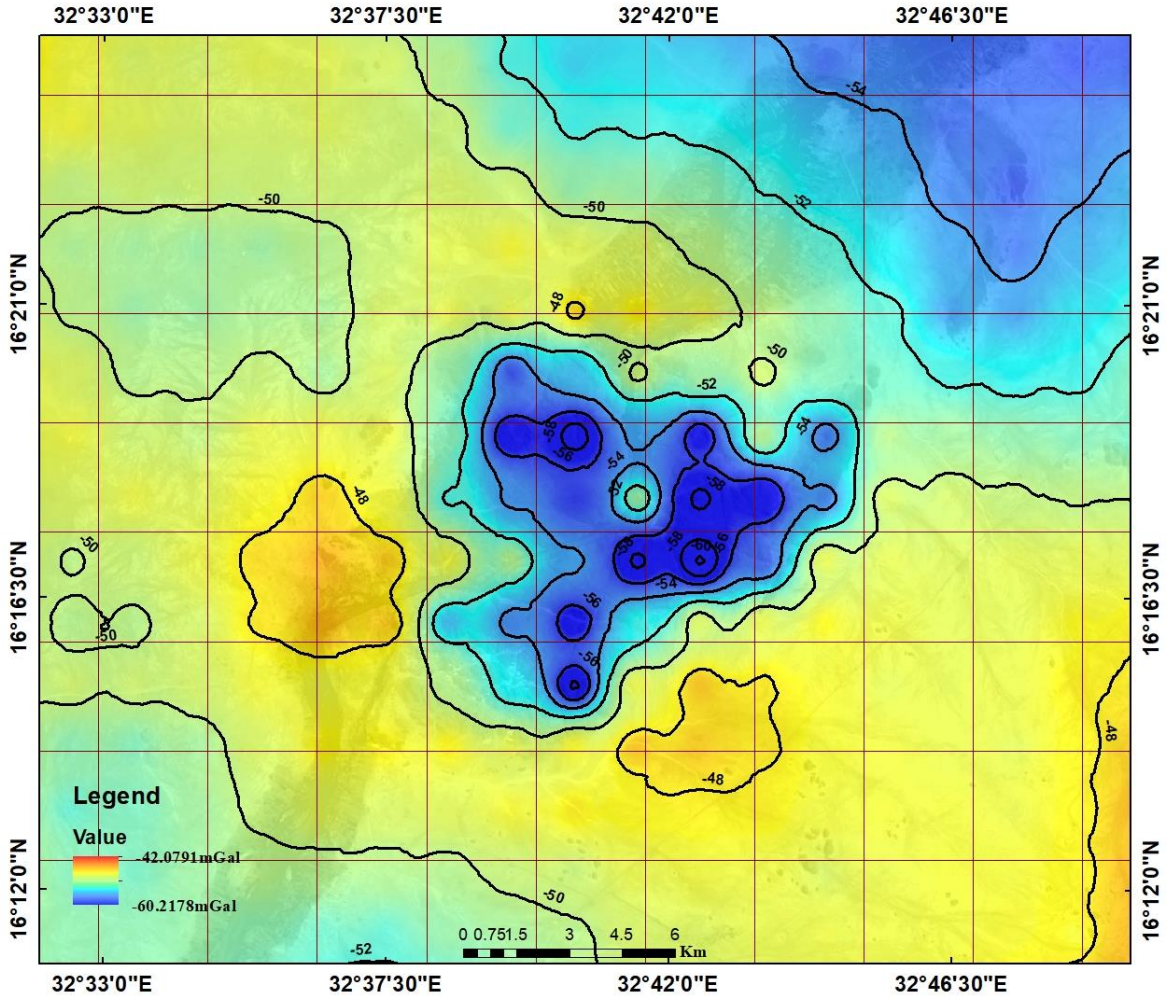

Figure (4.14): Bouguer gravity map of the study area, contour interval is 2mGal.

The obtained Bouguer anomaly map was visually interpreted in term of boundaries between units having different densities and thickness, due to variation in the gravity values. From the Bouguer anomaly map, the maximum

value is recorded over the exposed basement rocks of -48mGal, which is displayed in yellow color in the map. The low value of Bouguer anomaly is measured over the Shendi Formation in the northeastern part of the area and the sedimentary rocks in the southwestern part of the area and to the northeast of the volcanic plateau. The low values are displayed in blue color ranging in values between -51.08 to -55.45 mGal. The Sabaloka volcanic plateau have the minimum value in the area (-60.2178 mGal) although it is acidic volcanic rocks.

4.3.4.2 Regional- residual separation

The problem of the regional and residual anomalies arises in all geophysical methods which are based on measurements of a potential field. Basically, the question is that of separating a potential field into possible component parts and of ascribing separate geological causes to these parts. The determination of a satisfactory regional is a geological as well as a geophysical problem (Nettleton, 1954). Grant (1954*)* defined the regional gravity anomaly as "the field that is too broad to suggest the object of exploration and it is generally assumed to be smooth and regular, suggesting characteristically the field due to a deep-seated disturbance".

Nettleton (1954) adopted the following definition: "the regional is what you take out to make what is left looks like the structures". Paul (1967) defined it as “the regional field is the field that would be Produced when local anomalous masses are replaced by masses of the same density as that of the country rocks. This definition will smooth out the regional field sufficiently and also will signify the residuals as the field due to local mass distributions with densities equal to density contrasts i.e. true densities minus the densities of the surroundings".

Skeels (1967) defined the regional gravity as “the interpreter's concept of what the Bouguer gravity should be if the anomalies were not present" and the

residual gravity as "what remains of Bouguer gravity after subtraction of a smooth regional effect". Accordingly, the residual can be expressed as follows:

Residual gravity = Observed gravity - Regional gravity

Most other regional-residual anomaly separation techniques involve mathematical operations using a computer, the most common mathematical techniques are surface fitting and weighted averaging, which are used in the present study.

4.3.4.2.1 Weighted averaging

This is mathematical technique for the calculation the regional gravity anomaly from the flowing equation:

$$\overline{U} = \frac{U_{(x-1)} + U_{(x+1)} + U_{(y-1)} + U_{(y+1)}}{4r}$$

Where $\overline{U}$ is value of the regional , $U_{(x-1)}$ is Bouguer Anomaly of the point which fill in the x axis in the right of our point in the profile which we want to calculate the regional gravity anomaly to her, $U_{(x+1)}$is Bouguer Anomaly of the point which fill in the x axis in the left of our point in the profile which we want to calculate the regional gravity anomaly to her, $U_{(y-1)}$ is Bouguer Anomaly which fill in the y axis in the right of our point in the profile which we want to calculate the regional gravity anomaly to her $U_{(y+1)}$ is Bouguer Anomaly which fill in the y axis in the left of our point in the profile which we want to calculate the regional gravity anomaly to her, by this technique in our study we were calculating the regional gravity anomaly of all our profile and then calculated the residual gravity anomaly from the flowing equation:
Residual gravity = Observed gravity - Regional gravity.

4.3.4.2.2 Polynomial fitting

This is a pure analytical method in which matching of the regional by a polynomial surface of low order exposes the residual features as random errors (Telford et al., 1976). This method assumes the residuals to be random errors whose sum is zero. Thus the analytical residual is composed of positive and negative parts. The polynomial equation has the form:

$$y = a + bx + cx^2 + dx^3$$

Where a, b, c and d, are coefficients.

The polynomial order is the largest power of x in the equation. For fitting a data point (xi, yi), it assumes that all of the errors occur in the measured by values and there are no errors in the x values. Each value of X_r (r = 1, 2, 3, etc.) has a corresponding calculated y for the polynomial, and the difference between this regional and the observed value is called the residual Δr in Yr so,

$$\Delta r = (a + bxr + cxr^2 + ...).$$

The principle underlying the fitting of the polynomial to make the sum of the residual squares as small as possible by choosing appropriate values for a, b, c, etc.

High order polynomials may produce unwanted spikes between data points and then interpolation is necessary. Increasing the order of the polynomial can lessen the smoothing of the data. In extreme cases the order is equal to n-1 and the polynomial passes through each of the data points. This is called interpolating polynomial and there is no smoothing of data (Ahmed, 1994).

The results of computations of the regional and residual components using the averaging method were imported into the GIS environment for interpolation. This finally resulted in the preparation of regional gravity anomaly map with

counter interval of 1 mGal (Figure 4.15) and residual gravity anomaly map of the study area with counter interval of 1.3 mGal (Figure 4.16).

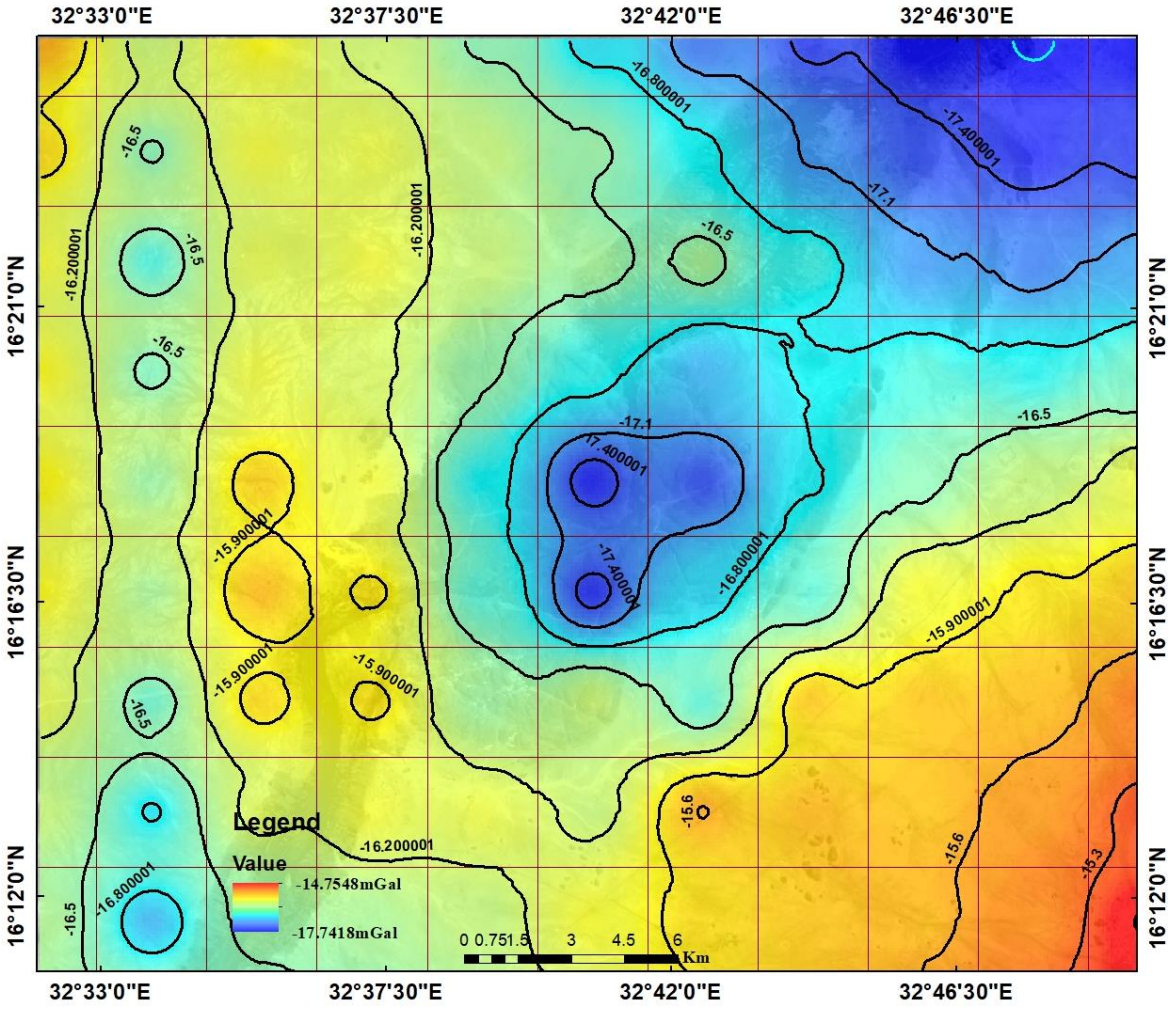

Figure (4.15): regional gravity anomaly map of the study area, contour interval is 1mGal.

The obtained regional gravity anomaly map was visually interpreted. The low values of the regional gravity anomaly were recorded for the Sabaloka volcanic plateau which has minimum value of -17.7 mGal and the sedimentary rocks of Shendi Basin and also there are low value in the western apart of the area, which was interpreted due to the existence of sedimentary rocks. The high value shown in the southeastern part of the study area is attributed to the intrusive granite which has maximum value of -14.7548 mGal. The contrary

rocks of gneisses and migmatites appear in high values around the volcanic plateau in the western and southeastern parts.

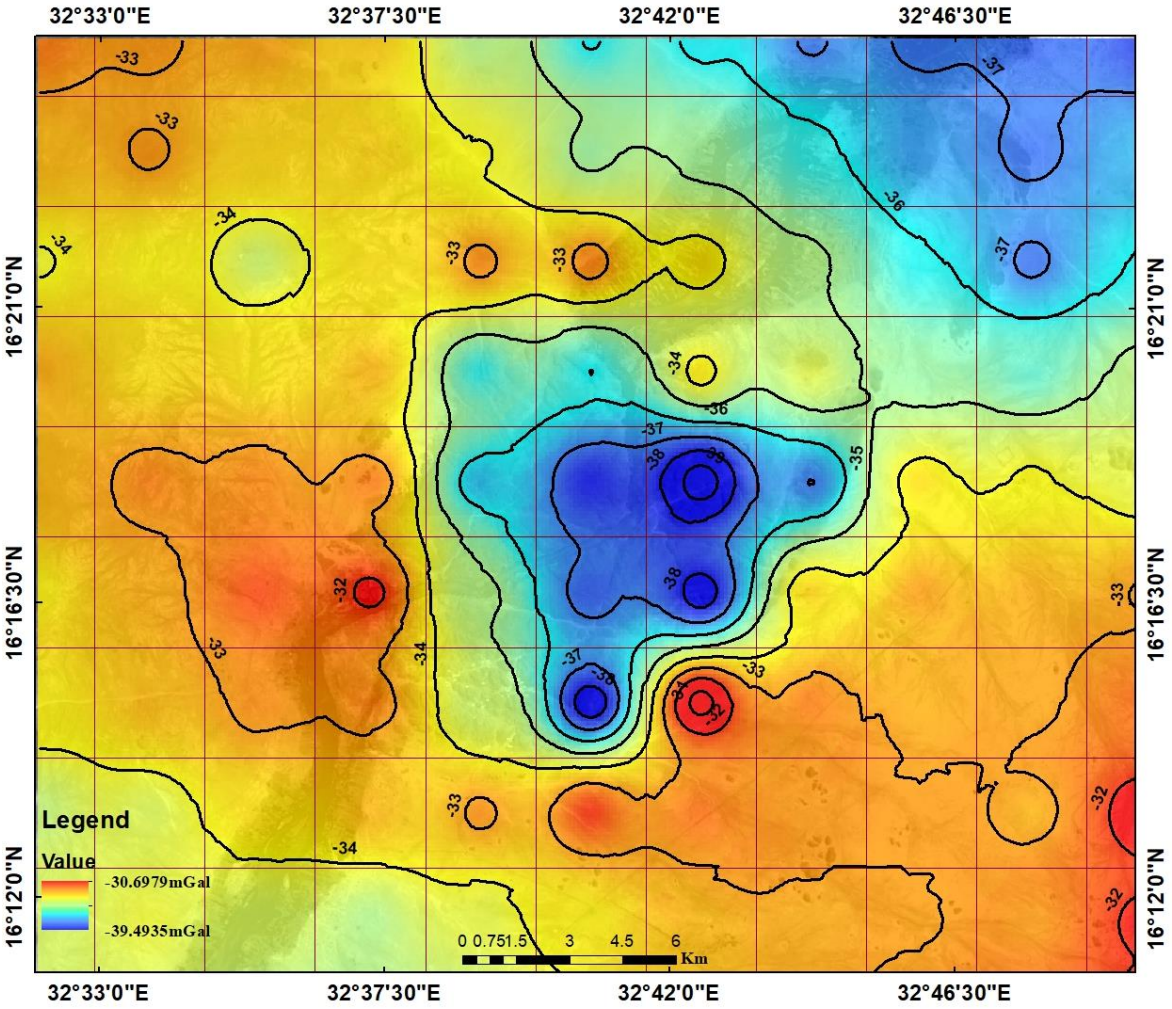

Figure (4.16): Residual gravity anomaly map of the study area, contour interval is 1.3mGal.

The low values of residual gravity anomaly recorded for the Sabaloka volcanic plateau which have minimum value -39.49 mGal and the sedimentary of Shendi Basin and also there are low value in the western apart of the area. It was attributed to sedimentary rocks. Higher values are shown in the southeastern part of the study area, where intrusive granite occupy the area with maximum value of -14.75 mGal). The contrary rocks appearing in high values around the volcanic plateau in the western part.

4.3.4.3 2.5D modeling

Quantitative interpretation (non-linear method) calls for approximation of the geological bodies, which are considered to be the gravity source, by assuming simple geometric model from which the theoretical gravity effect can be compared with the observed gravity data and the shape of the body can be changed (modified) to minimize the difference between the observed and the computed gravity effects, often by interactive and/or iterative computer inversion methods (Kearey and Brooks, 1988).

Gravity modelling is usually the final step in gravity interpretation and involves trying to determine the density, depth and geometry of one or more subsurface bodies. The modelling procedure commonly involves using a residual gravity anomaly. When modelling a residual gravity anomaly, the interpreter must use a density contrast between the body of interest and the surrounding material, while modelling Bouguer gravity anomalies; the density of the body is used. There are many different techniques available to perform the modelling procedure and they can be broken down into three main categories: 1) analytical solutions due to simple geometries, 2) forward modelling using 2-(two-dimensional), 2.5- (two and one-half dimensional) and 3-D (three-dimensional) irregularly shaped bodies, and 3) inverse modelling using 2-, 2.5- and 3-D irregularly shaped bodies. Most of these techniques involve iterative modelling (by the aid of a computer), where the gravitational field due to the model is calculated and compared to the observed or residual gravity anomalies.

the term ‘2.5D’ modeling of the anomalies. in this study was performed by Gravity Model program. The density measurements for all the sedimentary formations **(**2.67 g/cm^3**)** and the Basement rocks of the area **(**2.4 g/cm^3**)**. So the density contrast is **(**0.27g/cm^3**).**

the center of the profile is the volcanic plateau which The maximum thickness obtained for her by models is about 5km, and it show low ……. What?

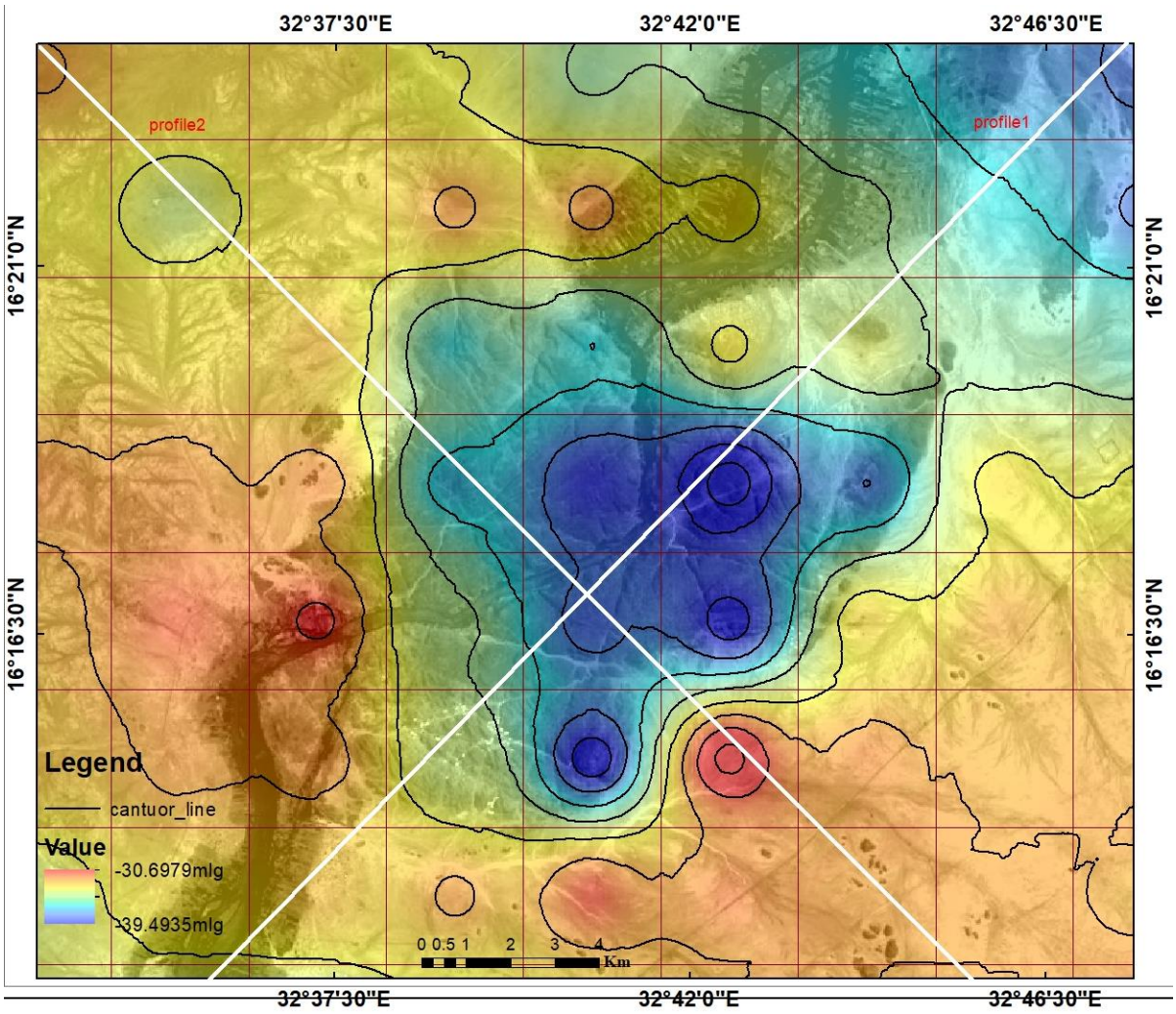

Figure (4.17): location map of the modeled profiles.

Profile 1

The profile runs in the NE-SW direction. The gravity field along the profile represents residual gravity anomaly**,** with low gravity anomaly in the center and northern east and southern west part of the model flanked by two highs of different amplitudes Figure (4.19), the northern east part is Shendi Basin, the sedimentary thickness is about 7.5km it shows low value, while the

sedimentary in the southern west show low value but higher than Shendi Basin that due to the porosity, they have the same thickness, the porosity in Shendi Basin is higher, the fourth point in the profile is Umm Marahik sediment which preserve by Umm Marahik fault it show high reading if we compare her with the sedimentary along the profile, the thickness of sedimentary is about 2.5km, the down throw of the rotation fault obtained by models is about 1.5km, hence the low reading due to the small thickness of the sediment, the center of the profile is the volcanic plateau, the thickness of the volcanism is show high, it is about 5km obtained by models and the mantel is far away ,the root of the volcanism it a big that a signaled by AIRY when he said "the inner part of the weight of the mountains cannot be hollow, rather the excess weight of the mountains is compensated or balanced by lighter material ,bellow ,he assumes that the light sial is floating on heavier sima. hence Himalayas are floating in denser glassy magma. Airy further assumed that Himalaya are floating in the denser magma with their maximum portion sunk in the magma in the same away as a boat floats in water with it is maximum part sunk in the water .in fact this concept involves the principle of flotation .if we assume the average density of the crust as 2.67 and that of substratum as 3.0,so,for every one part of the crust to remain above the substratum ,nine part of the crust must be in substratum according to the principle of flotation .he further claims that density zone not change with depth, that is"uniform density with varying thickness" . that interpreted the low reading of the gravity in Sabaloka igneous complex , the high value it is the basement ,the exposed basement show higher value along the profile, there are two major normal faults show in the model.

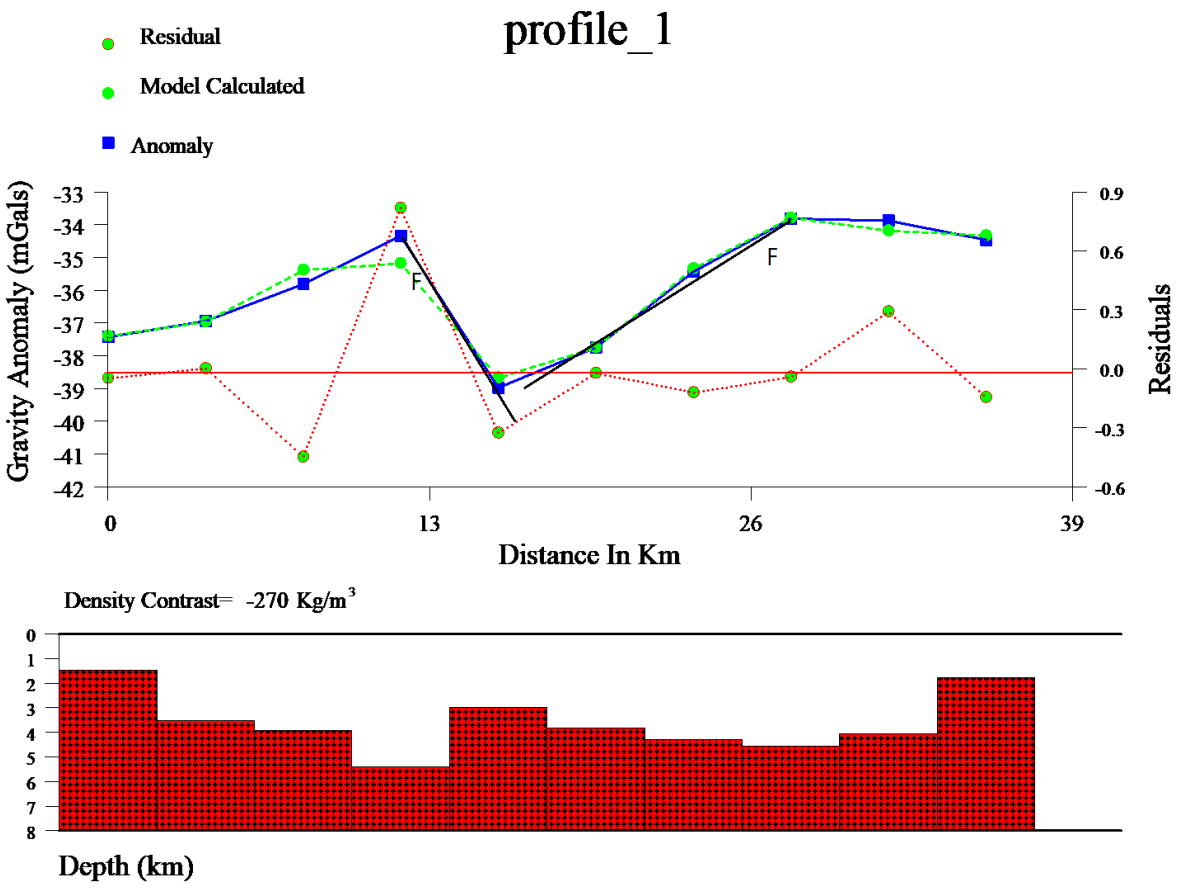

Figure (4.18): Residual anomalies Vs distance of the profile 1, F stand for fault.

Profile 2

The profile runs in the NW-SE direction. The gravity field along the profile represents residual gravity anomaly Figure (4.20)**,** with low gravity anomaly in the center, it is the volcanic plateau of the Sabaloka igneous complex. The exposed basement along the profile from NW-SE given high reading. the sediment in the northern west of the plateau shows low reading, the porosity is low, there are two major normal faults show in the model, in the map the fault appears by closed the contour line of the gravity

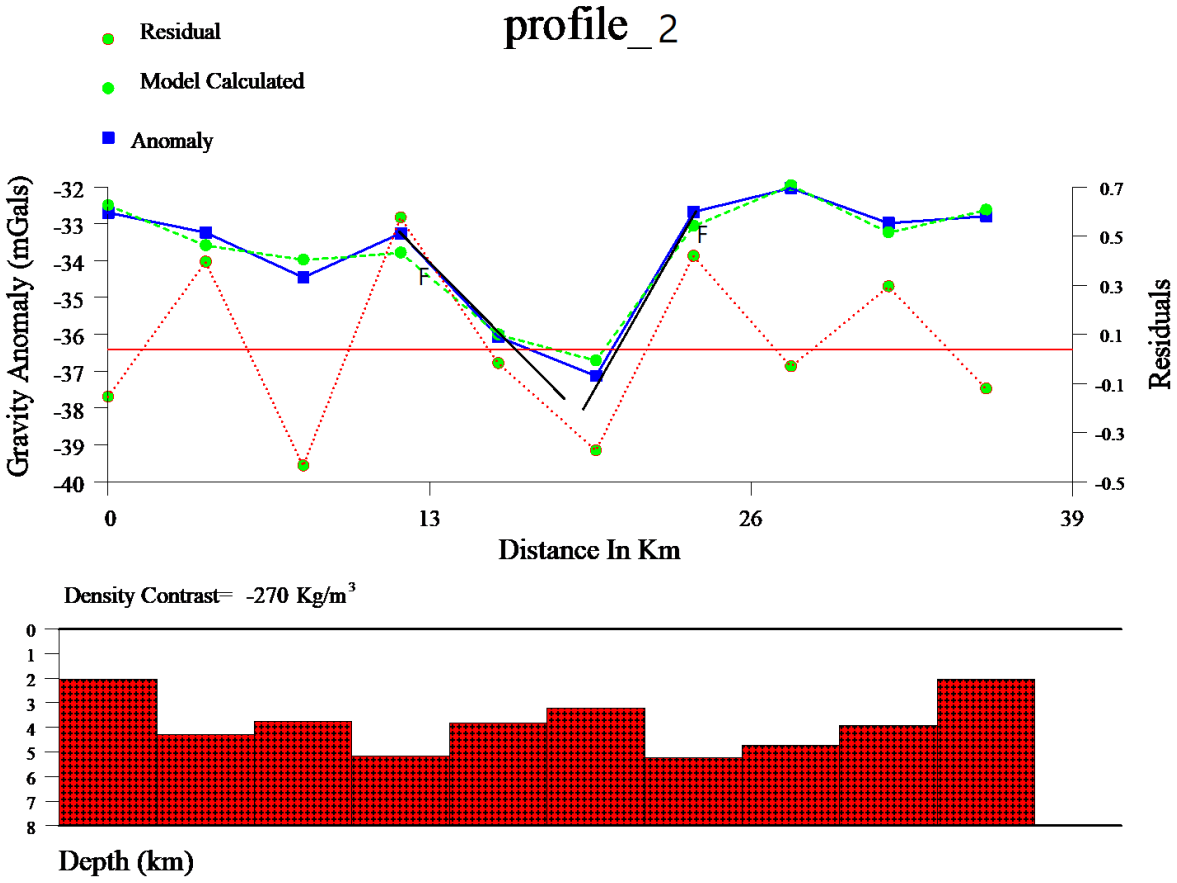

Figure (4.19): Residual anomalies Vs distance of the profile 1, F stand for Fault.

CHAPTER FIVE: CONCLUSION AND RECOMMENDATIONS

5.1 Conclusions

This work covers a large area of the Precambrian rocks in the Sabaloka inlier. The current work represents an attempt to map the area through the use of digital image processing techniques of satellite data and satellite gravity.

Different digital image processing techniques have been applied to Landsat 8 OLI image in order to increase the discrimination between various lithological units. Image sharpening was performed to enhance the spatial resolution of the image for more detailed information. Contrast stretching was applied, after the various digital processing procedures to produce more interpretable images. The Principal Component Analysis transformation yield saturated images and resulted in more interpretable image than the original data. Several ratio images were prepared, combined together and displayed as RGB color images.

All the images, obtained through the above mentioned processes, have been used simultaneously to produce the geological map of the study area in the GIS environment.

Gravity point data was used in the present study. Polynomial fitting was used in order to separate the regional from the residual component of the gravity. This technique gave negative residual anomaly over Sabaloka Igneous Complex. Bouguer residual and regional gravity map were produced for the study area. The negative residual anomaly over Sabaloka Igneous Complex is attributed to the volcanic rocks which increase the thickness of the earth crust. Two profiles were constructed across the residual gravity map in an approximately, NE-SW and NW-SE directions cutting the most prominent anomalies in the area. Normal fault is the dominant fault type. The fault of Umm Marahik is not clear in the model because the thickness of the sediment is not so pig.

The outcome of the present study was a model of the subsurface geology of the study area based on the residual gravity map of the above-mentioned two profiles.

There are variations in the gravity value in the study area. the complex shows low value due to the large thickness, in other part of the area the sedimentary rocks also shows low reading, while the basement either exposed or occurred in shallow depth records high readings.

5.2 Recommendations

1. The present work generated new information about the Sabaloka inlier. The conducted gravity investigations are not adequate and still more information can be obtained about the subsurface structure. Accordingly, more detailed gravity study is recommended to provide new information about the structure history of the area.

2. Some companies are exploiting the mineral resource of the area, i.e. rocks as building materials. Care must be takes when exploiting the resource so as not to destruct the geological environment of the area.

3. Stop the military monopoly of some parts of the region, which hinder the fieldwork of students.

4. The area is one of the most important geological site in the country and may be in the world that is characterized by a variety of rock units and structures. It represents an ideal area of field training for students. Accordingly, the area must be preserved as a geo-park.

5. The geopark may activate the tourism in the area. This may be supported by the existence of the sixth cataract (Sabaloka cataract), and the development of the economic return of the country.

References

Abdel Rahman, El. M. (1993): Geochemical and Geotectonic Control. G.W einert, Offset druck Eriei Saalburgst. 3, 1000 Berlin 42 .

Abdelsalam, et.al (2003): Neoproterozoic deformation in the northeastern part of the Saharan Metacraton, northern Sudan. Pre. Res. 123, 203-221.

Ahmed, F. (1968): Geology of Jebel Qeili, Butana and Jebel Sileitat-es-Sufr Igneous Complex, Nile Valley, Central Sudan: M. Sc. Thesis, Univ. of Khartoum .

Ahmed, M. M., (1994): Geophysical Study of the Central Sudan Granulites. M.Sc. Thesis, Dept. of Geol., Univ. of Khartoum.

Almond, D.C and Ahmed, F., (1993): Field Guide to the Geology of the Sabaloka Inlier, Central Sudan. Khartoum University press, Khartoum, Sudan .

Almond, D.C., (1977): The Sabaloka Igneous Complex, Sudan. Philosophical transaction of Royal Society of London, A, 287,595-633 .

Almond, D.C., (1980): Pre Cambrian Events at Sabaloka near Khartoum and Their Significance in the Chronology of the Basement Complex of North Sudan. Precambrian Res., 13:43-62 .

Almond, D.C., Harris, N.B.W. and Evans, J.A (1989): Natural glass dyke from Sabaloka and its relevance to the history of Younger Granites in Sudan. The Journal of the University of Kuwait (Science), 16, 425-432 .

Tapley, B.D and. Kim, M.C, Chapter 10 Applications to Geodesy. In: LEE-LUENG, F. and ANNY, C. (eds.) International Geophysics. Academic Press, .2001

Berry L., Whiteman A. J. (1968): The Nile in the Sudan. Geogr. J. 134: 1-37 .

Bertini, F., Brand, O., Carlier, S. Del Bello,U. (2012): Sentineal- 2,European Space Agency.

Hwang, C., E-C. Kao and B. Parsons. Global derivation of marine gravity anomalies from Seasat, Geosat, ERS-1 and TOPEX/POSEIDON altimeter data. Geophysical Journal international, 134: 449-459, 1998 .

Sandwell D.T and Smith, W.H.F., (1997): Marine gravity anomaly from Geosat and ERS-1 satellite altimetry. Journal of geophysical research-all series, 102: 10-10 .

Dawoud, A. S and Schulz- Dobric, B., (1993): PT Condition of Pan African Granulite Facies Metamorphism in Sabaloka Inlier North of Khartoum, Sudan. Geo Sci.Res. In North East (ed) Thoreweihe and Schandelemeier

Dawoud, A.S and Sadig, A.A., (1988): Structural and Gravity Evidence of an Uplifted Pan African Terrain in Sabaloka Inlier. J. Africa. Earth Science, 7,787-794 .

Dawoud, A.S., (1970): A Geological and Geophysical Study of the Area South-East of Qerri Station, Eastern Sabaloka, North Khartoum Province, Sudan. Thesis, Univ. of Khartoum .

Delany F. M. (1960): Sudan. Lexique Strat. Int. 6: 77-105. C. R. 21 st Int. Geol. Congr. Copenhagen .

Delany, F. M. (1955): Ring structures in the northern Sudan. Eclogae Geol. Helv., v. 48, p. 133-148 .

Drury, S.A., (1993): Image interpretation in geolgy.-2nd ed., -283 pp., London (Chapman and Hall) .

Eby, G.N., (1990): The A-type gramtoids: A review of their occurrence and chemical charactenstics and speculations on theIr petrogenesIs. In: A.R.

Woolley and M. Ross (EdItors), alkaline igneous rocks and carbonatites. Lithos, 26: 115-134 .

Gupta, R. P. (2003): Remote Sensing Geology. Second Edition, Berlin. 655 pp .

Harris, N.B.W., Duyverman, H.J. and Almond, D.C., (1983): The trace element and isotope geochemistry of the Sabaloka Igneous Complex, Sudan. Journal of the Geological Society of London, 140, 245-256.

http://www.jpl.nasa.gov/missions.

http://www.nasa.gov.

Keenan, P. (1997): Using a GIS as a DSS generator. University College Dublin, Faculty of Commerce, Department of Management Information Systems, 25 pp .

Key RM, Charley T J, Hackman BD, Wilkinson AF, Rundle CC. (1989): Superimposed Upper Proterozoic collision-controlled orogenies in the Mozambique orogenic belt of Klemenic, P.M. (1987): Variable intra-plate igneous activity in central and north-east Sudan. Journal ofAf rican Earth Sciences, 6, 465-474 .

Kheiralla, M. K. (1966): A study of the Nubian Sandstone Formation of the Nile Valley between 14 N and 17 42 N with the reference to the ground-water geology. M. Sc. Thesis, Univ. of Khartoum, (Unpublished thesis).

Kroner, A. Stern, R.J. Dawoud, A.S Composition. And Reischman, T., (1987): The Pan African Continental Margin in North Eastern Africa. Evidence from Geochronological Study of Granulite at Sabaloka. Sudan. Earth Plant- Sci.Lett, 85, 91-104 .

Lasselle. M.C and Wones, D.R., (1979): Characteristics and origin of anorogenic granites. Geol. Soc. Am. Abstr. Programs, II: 468 .

Lille sand, T.M., Kiefer, R.W., and Chipman, J.W., (2003): Remote sensing and image interpretation (5th edition). John Wiley & Sons, 111 River Street, Hoboken, NJ, 070305774 (201) 748-668 .

Liu, J. G and Mason, P. J., (2009): Essential Image Processing and GIS for Remote Sensing, John Wiley & Sons Ltd, Oxford, UK

Lo. C.P., (1995): Automated population and dwelling unit estimation from high-resolution satellite images: a GIS approach. Internat. J. Remote Sensing, 16-1, 17-34 .

Nabigian, M.N., Andr, M.E., Grauch, V.J.S., Hansen, R.O., Lafehr,T.R. Oerson,Y. Li, Peirce, W.C. J.W. Phillips, J.D. and Runder, M.E. (2005) :75th Anniversary - Historical development of the gravity method in exploration. Geophysics, 70, 63ND-89ND.

Medan, A.H. (1975): Nubian Sandstone (Sudan). Distribution and typical. Section. American Association of Petroleum Geologists, 59, 345- 347 .

Mosley PN. (1993): Geological evolution of the Late Proterozoic "Mozambique Belt" of Kenya. Tectonophysics 221:223-50

Mujjo, C.P., (2010): Application of remote sensing for gold exploration in the nuba mountains, Sudan. M S.C thesis, Bowling Green State University .

Nava lung, R.R., Jayaraman, V., and Roy, P. S., (2007): Remote sensing applications: An overview, indian space programme, current science, vol. 93, and no. 12, 25 december 2007 .

Nettleton, L. L., (1954): Regional’s, residuals and structures. Geophysics, 19, 01, 01.

Olson, C. E. (1960): Elements of Photographic Interpretation Common to Several Sensors," photographic engineering, vol. 26, no. 4, pp. 651-656 .

Omer, M.K. (1975): Genesis and diagenesis of the Nubian Sandstone formation in Khartoum Province. Bulletin of Department of Geology and Mineral Resources, Sudan, 27, 48 pp .

Omer, M.K. (1978): Geologies des gres de Nubie du Soudan central, oriental et septentrional. Genese, diagenese et paleogeographie. These de Doctorat d'Etat, University de Grenoble, France, 213 pp .

Paul, M. K., (1967): A method for computing residual anomalies from Bouguer gravity maps by applying relaxation technique. Geophysics, 32, 04, 708 – 7.

Prasad, G., Lejal-Nicol, A. and Vaudois-Mieja, N. (1986): A Tertiary age for Upper Nubian Sandstone Formation, Central sudan. American Association of Petroleum Geologists Bulletin, 70, 138-142 .

Sabin's, F. Floyd (1999): Remote Sensing for Mineral Exploration. Ore Geol. Rev., 14. Elsevier Science. Sci., 22, 108- 125.

Steels, D. C., (1967): What is residual gravity? Geophysics, 32, 5, 872.

Stern R.J, (1994): Arc assembly and continental collision in the Neoproterozoic East African Orogen: implications for the consolidation of Gondwanaland. Annual Reviews Earth Planetary Sciences 22: 319-35 .

Greicius, T. GRACE mission overview [online]. NASA. Available at: http://www.nasan.gov/mission_pages/Grace/overview/index /html [accessed 8 .April 2014]

Telford, W. M., Geldart, L. P., Sheriff, R. E. and Keys, D. A., (1976): Applied Geophysics. Cambridge University Press, 860 pp.

Vail, J. R. (1985): Alkaline ring complexes in Sudan. Dept. Geol. Portsmouth Polytechnic, U.K. Vol.13, 51-59 .

Vearncombe JR. (1983): A proposed continental margin in the Precambrian of western Kenya. Geol. Rundsch. 72:663-70.

Venkata Dasu M. A. ; Shaik, F. and Abd El-Rahim, B. (2011): An Application of Decorrelation and Linear Contrast Stretching Methods on Satellite Images. VSRD-IJEECE, Vol. 1. 402.